An Unsplit Monte-Carlo scheme for the resolution of the linear Boltzmann equation coupled to (stiff) Bateman equations

Adrien Bernede, Gaël Poëtte

An Unsplit Monte-Carlo scheme for the resolution of the linear Boltzmann equation coupled to (stiff) Bateman equations

Adrien Bernede[1], Gaël Poëtte[1]
[1] *CEA, DAM, DIF, F-91297 Arpajon, France*

Abstract

In this paper, we are interested in the resolution of the time-dependent problem of particle transport in a media whose composition evolves with time due to interactions, the only constraint being the use of Monte-Carlo (MC) scheme for the transport phase. A common resolution strategy consists in a splitting between the MC/transport phase and the time discretization scheme/matter evolution phase. After going over and illustrating the main drawbacks of split schemes in a simplified configuration (monokinetic/monocomposition problem), we progressively build a new Unsplit MC (UMC) scheme improving the accuracy of the solutions, avoiding numerical instabilities, and less sensitive to time discretization. The new scheme needs two key ingredients: an Unsplit MC solver and a specific change of variable implying an *on the fly* resolution of a system of ODEs for each MC particle in order to describe along their flight path the time evolution of the matter.

Key words: Transport, Bateman equations, Monte-Carlo, Ordinary Differential Equation, Coupling, splitting, Numerical scheme, Burn-up

1. Introduction

In this paper, we are interested in the resolution of the time-dependent problem of particle transport in a media whose composition evolves with time due to particle interactions. We suppose transport to be driven by the linear equation (1a) for particles p having position $x \in \mathbb{R}^3$, velocity $v \in \mathbb{R}_+$, direction $\omega \in [0, 2\pi] \times [0, \pi]$, at time $t \in \mathbb{R}^+$ and where the quantity $u(x, t, v, \omega)$ is the density of presence of the particles p at (x, t, v, ω). The interaction of particles with matter is described through macroscopic characteristics $(\sigma_\alpha)_{\alpha\in\{t,s,a\}}$ (1c) with $\sigma_t = \sigma_s + \sigma_a$ the total interaction probability being the sum of scattering and absorption probabilities. For matter evolution, we consider the decomposition of the latter macroscopic characteristics into constant microscopic parameters $(\sigma_\alpha^m)_{\alpha\in\{t,s,a\}}$ and vector of material densities η (1b). We assume that time variation of the material density η can be accurately modeled by Bateman equations [10] (1d) where Σ^R denotes the matrix of reaction rates. As a result, problem (1) is non-linear and strongly coupled:

$$\begin{cases} \partial_t u(x,t,v,\omega) + v\omega\nabla u(x,t,v,\omega) + v\sigma_t(\eta(x,t),v)u(x,t,v,\omega) \\ = \iint v\sigma_s(\eta(x,t),\omega,\omega',v,v')u(x,t,v',\omega')\,\mathrm{d}\omega'\,\mathrm{d}v', & (1a) \\ \eta(x,t) = \left(\eta^1(x,t),...,\eta^M(x,t)\right)^t, & (1b) \\ \sigma_\alpha(\eta(x,t),v) = \sum_{m=1}^{M} \sigma_\alpha^m(v)\eta^m(x,t), \forall\alpha\in\{t,s\}, & (1c) \\ \partial_t\eta(x,t) = \iint \Sigma^R(\eta(x,t),v)vu(x,t,v,\omega)\,\mathrm{d}\omega\,\mathrm{d}v. & (1d) \end{cases}$$

Email address: adrien.bernede@cea.fr, gael.poette@cea.fr (Adrien Bernede[1], Gaël Poëtte[1]).

Under this general form, system (1) can be used in many fields of applications. The Bateman counterpart (1d) may be considered as a particular case of the Lotka-Volterra system (see [23]) in which we only keep the strong coupling term. However this simplification is sufficient to emphasize and study the numerical issues of interest in this paper (see section 2 on the following page). Amongst the applications (non exhaustive list), one can quote biology [23] with population dynamics, or physics [5, 13, 14, 8] with burn-up computations in neutronics. In the following, we refer to publications dealing with burn-up applications as numerical studies have mainly been carried in this context [5, 13, 14, 8]. Of course, the numerical methodology we develop in this paper is very general and can be used whatever the application domain.

We aim at solving transport phase (1a) using a Monte-Carlo (MC) scheme [15, 25, 16]. This MC scheme will consequently be coupled with a time discretization solver for the Bateman equation (1d). MC methods applied to transport equations present some valuable advantages: the rate of convergence is independent of the solution smoothness and the potentially high problem dimension (i.e. here dimension $7 = 3(x) + 1(t) + 1(v) + 2(\omega)$) [25, 15, 16, 3]. MC methods also allow minimum hypothesis on the closure of the system and on the preprocessing of the data (σ_α^m) [25, 16]. [1]

The common resolution strategy consists in a splitting between the MC/transport phase and the time discretization scheme/Bateman phase. Concerning the Bateman counterpart of system (1) several time discretization schemes can be applied such as Runge-Kutta 4, explicit or implicit Euler, predictor-corrector etc. The reader may refer to [5, 13, 8, 7] and the reference therein for complete descriptions of the commonly used schemes applied to burnup problems. One of the aim of this paper is precisely to analyse and understand the pros and cons of these strategies by applying them on a test-case allowing to isolate the difficulty and emphasize the limitations arising when applying such splitting. This will be the purpose of section 2 on the next page in which we simplify the system (1) (monokinetic transport and degenerate Bateman equations) and build an analytical solution for the strongly coupled system under several general hypothesis. To our knowledge, such an analytical solution has never been stated. It allows for a complete quantitative study of the numerical schemes at use in this paper and presents also an advantage in term of verification (as in V&V, [1]) of a simulation code for whoever wants to develop the numerical resolution of system (1).

In section 3 on page 8, we suggest a new MC scheme aiming at decreasing the previously described undesired effects (see section 2) which we expect to be mainly due to a splitting of operators. In order to build this scheme, we need to rely on a Unsplit Monte-Carlo (UMC) scheme alieviating the hypothesis of constant characteristics with respect to time. After reminding how MC scheme can feature non-constant coefficients in section 3.1 on page 8, we detail how we incorporate the Bateman resolution of (1d) within the evolution of each MC particle (section 3.2 on page 9). Doing so we provide a transport phase which depend on matter evolution through justified hypothesis. Care will be taken in order to emphasize the key steps of our algorithm together with the experimental verification of its mathematical/numerical properties on a simplified version of (1).

The UMC scheme was first presented on a simplified problem. Sections 4 to 5 are then dedicated at progressively relieving the hypothesis and approximations stated in sections 2 to 3. Section 4 on page 14 complexifies the problem coupling monokinetic transport with (non degenerate) Bateman equations. This new step introduces a first numerical difficulty concerning the application of the UMC scheme we suggest: the need for an ODE solver for solving on the fly the collisional couterpart of the transport equation along the flight path of the MC particle transport. Section 5 on page 21 presents the complete methodology we apply in order to build our UMC scheme in the general case (energy/velocity dependence and Bateman equations). It relies on two key ingredients: a particular change of variable, closely related to Quasi-Static methods [11, 12, 4, 18] with dependences with respect to time, space and energy, the resolution of balanced transport equation with time dependent characteristics.

The constants $((\sigma_\alpha)_{\alpha\in\{s,t,a\}}$ are not physical and have been chosen in order to emphasize numerical issues (and not physical ones). They are the simplest possible for the sake of reproducibility of the results. Of course, our method still apply for more realistic constants.

As a conclusion, in section 7 on page 28, we will briefly remind the main aspects of the paper, present future works and the expectations for our UMC scheme in term of physical applications (real constants) and concisely hint at some High Performance Computing (HPC) considerations.

Concerning the classical numerical methods used in the different phases (MC schemes for transport equation and time discretization schemes for the Bateman phase), we chose to detail their specifications in the appendix A. This appendix is also introducing some notations and accurately details the schemes for the sake of an eventual reproduction of the results presented in this paper.

[1] Other solvers could be used and the algorithms therein this paper may be adapted for them (S_n solvers, P_n solvers, ...) but this is beyond the motivations of this paper.

2. A reduced homogeneous problem to highlight weaknesses of usual schemes

In this section, our aim is to pedagogically put forward the limitations of solvers involving splitting between schemes when coupling transport equation (solved using MC method), to a Bateman system. To do so, we begin making some simplifications allowing the construction of an analytical solution for the strongly coupled system without loss of generality. Then we perform some deepened convergence studies with the common numerical schemes of the literature. Note that in this paper, we obviously do not test every existing schemes but only the ones we consider relevant to serve our purpose. For complementary studies, we refer to [5, 13, 8, 7] with applications to burnup problems. Note that this section can also be considered as a new and original way (using a simple strongly nonlinear coupled system rather than a complex test problem) to present similar results as in [8, 7]: we repeatedly refer to their work in the following.

First, considering the numerical difficulties we want to highlight in this paper, we can assume a monokinetic particle transport equation, i.e. $u(x,t,v,\omega) = u(x,t,\omega)$. Besides, we use the classical decomposition of the (here monokinetic) scattering term as $\sigma_s(x,t,\omega',\omega) = \sigma_s(x,t)P_s(\omega',\omega)$ where $P_s(\omega',\omega)$ is the probability for a particle p having direction ω' to get out of an interaction with direction ω (i.e. $\forall\omega, \int P_s(\omega',\omega)\,\mathrm{d}\omega' = 1$). Finally, it is not restrictive to consider the simplest Bateman equation (scalar $\eta = \eta^1$) where the reaction matrix Σ^R degenerates to a scalar reaction rate σ_R^m. The simplified system, still stronglycoupled, is thus a 2-equations system written for the sake of conciseness without the dependences with respect to x, t, ω:

$$\begin{cases} \partial_t u + v\omega\nabla u + v\sigma_t^m \eta u = v\sigma_s^m \eta \displaystyle\int P_s u\,\mathrm{d}\omega', & \text{(2a)} \\ \partial_t \eta = \eta\sigma_R^m v \displaystyle\int u\,\mathrm{d}\omega. & \text{(2b)} \end{cases}$$

Note that the latter simplified system is still general in the sense we can still explore very different kinds of regime (absorbing, multiplicative etc.) by only changing the values of $(\sigma_\alpha)_{\alpha\in\{s,t,R\}}$. This will be emphasized in the following sections.

We are now going to build an analytical solution for the strongly coupled simplified system (2) in the homogeneous case. To our knowledge, such analytical solution is original and will be intensively used (as long as we consider one group and one material) in order to perform quantitative convergence studies and analysis. It can also be very convenient in term of code verification for whoever needs to develop solvers/schemes such as the ones presented in the following [1].

2.1. *Analytical solution for reduced homogeneous test-problem (2)*

As we are focusing on time evolution of the solution, it is enough considering a spatially homogeneous solution of system (2), i.e. such that $u(x,t,\omega) = u(t,\omega)$. We write $U(t) = \int u(t,\omega)\,\mathrm{d}\omega$ such that with unknowns $(U(t),\eta(t))$, (2) becomes

$$\begin{cases} \partial_t U(t) + v\underbrace{(\sigma_t^m - \sigma_s^m)}_{\sigma_a^m}\eta(t)U(t) = 0, \\ \partial_t \eta(t) = \sigma_R^m \eta(t) v U(t). \end{cases} \tag{3}$$

In the above formulation, we used the fact that $\int P_s(\omega',\omega)\,\mathrm{d}\omega = 1$ so that

$$\begin{aligned} \int\int P_s(\omega',\omega)u(t,\omega')\,\mathrm{d}\omega'\,\mathrm{d}\omega &= \int u(t,\omega')\int P_s(\omega',\omega)\,\mathrm{d}\omega\,\mathrm{d}\omega', \\ &= \int u(t,\omega')\,\mathrm{d}\omega', \\ &= U(t). \end{aligned} \tag{4}$$

In order to build the analytical solution for system (3), first remark that the quantity $\sigma_R^m U(t) + \sigma_a^m \eta(t)$ is conserved, i.e.

$$\partial_t\left(\sigma_R^m U(t) + \sigma_a^m \eta(t)\right) = 0,$$

so that

$$U(t) = U_0 + \frac{\sigma_a^m}{\sigma_R^m}(\eta_0 - \eta(t)).$$

Now plugging the above expression in the first equation of (3) results in an ODE of unknown η

$$\partial_t \eta(t) = v(\sigma_R^m U_0 + \sigma_a^m \eta_0)\eta(t) - v\sigma_a^m \eta^2(t),$$

which can be solved analytically. Once every computation performed, we get

$$U(t) = \frac{(\sigma_R^m U_0 + \eta_0 \sigma_a^m) U_0}{\sigma_R^m U_0 + \eta_0 \sigma_a^m e^{v(\sigma_R^m U_0 + \eta_0 v \sigma_a^m)t}}, \ \eta(t) = \frac{(\sigma_R^m U_0 + \eta_0 \sigma_a^m)\eta_0}{\sigma_R^m U_0 e^{-v(\sigma_R^m U_0 + \eta_0 v \sigma_a^m)t} + \eta_0 \sigma_a^m}. \tag{5}$$

We will now use this analytical solution as a tool to test and compare, in different regimes, several solvers featuring MC schemes (for the transport phase) and some time discretization schemes (for the Bateman phase). Of course, such analytical solution only allows detecting numerical scheme lacks with respect to time discretization (the geometrical/spatial aspect can be preponderant in many applications, see burnup applications [5, 13, 8, 7] for example). However, in this paper we focus on temporal aspects only.

2.2. *Stiff reaction rate test-problem 1g1r$_\varepsilon$-h*

Let us introduce here our first test-problem which numerical values are given in table 1. We denote it by 1g1r$_\varepsilon$-h since it is monokinetic (1g for one group), the Bateman equation is scalar (1r for one reaction) and homogeneous (h, i.e. we have only one cell in an infinite medium). The subscript ε refers to the stiffness of the problem $\sigma_R^m = -\varepsilon$.

U_0	η_0	v	σ_t^m	σ_s^m	σ_R^m	ε	left BC	right BC
1.00	1.00	1.00	1.00	$1+\varepsilon$	$-\varepsilon$	0.15	specular	specular

Fig. 1. Parameters for the test 1g1r$_\varepsilon$-h.

For this problem, the reaction rate $\sigma_R^m = -\varepsilon$ being negative, the matter density decreases to zero as the flux of particles passes through it. Besides, as $\sigma_s > \sigma_t$, the problem is multiplicative for the particles. Consequently, the particle density increases with respect to time until the medium tends to a 'vacuum' ($\eta \to 0 \Longrightarrow \sigma_t \to 0$). The analytical solution for this problem is presented in fig. 2 on the next page (reference black curve). For the numerical resolution of system (2) in configuration described in table 1 we rely on two schemes :

- the MC scheme of appendix A.3 for solving the transport counterpart,
- the time discretization schemes described in the hereafter for the Bateman one.

2.3. *Application of split MC/explicit Euler scheme for the Bateman counterpart on problem 1g1r$_{\varepsilon=0.15}$-h*

The application of the split MC/explicit Euler scheme with track length estimator [25, 15, 16, 3] consists in integrating (2b) on a time step Δt so that (2b) becomes

$$\eta^{n+1} = \eta^n + v\sigma_R^m \int_{t^n}^{t^{n+1}} \eta(s) \int u(s,\omega)\,\mathrm{d}\omega\,\mathrm{d}s,$$

and then choosing

$$\int_{t^n}^{t^{n+1}} \eta(s) \int u(s,\omega)\,\mathrm{d}\omega\,\mathrm{d}s \approx \eta^n \int_{t^n}^{t^{n+1}} \int u(s,\omega)\,\mathrm{d}\omega\,\mathrm{d}s.$$

so that the scheme is explicit for the matter density η but not for the density of particles u. The integral $\int_{t^n}^{t^{n+1}} \int u(s,\omega)\,\mathrm{d}\omega\,\mathrm{d}s$ is evaluated thanks to the track length estimator [25, 15, 16, 3] of the MC scheme in a previous transport phase. Note that a comparable behavior is obtained with a purely explicit scheme (i.e. explicit also on the particle density u), i.e. if we approximate

$$\int_{t^n}^{t^{n+1}} \eta(s) \int u(s,\omega)\,\mathrm{d}\omega\,\mathrm{d}s \approx \Delta t \eta^n \int u(t^n,\omega)\,\mathrm{d}\omega.$$

The red curves in fig. 2 on the next page correspond to problem 1g1r$_{\varepsilon=0.15}$-h approached with the non-analog MC scheme for transport (see appendix A.3) coupled to the explicit Euler scheme described below, with $N_{MC} = 1000$ and $\Delta t = 5$.

Fig. 2 on the following page shows that for such parameters, the stiff reaction rate (or the large time step) leads to non physical values, i.e. $\eta < 0$. This also implies an oscillatory behavior of the quantities $(U(t), \eta(t))$ with respect to time even if the stationary states are accurately captured. This numerical instability problem can be compared to the one encountered for example in Xenon oscillations problem in burn-up studies [14, 8] and will motivate some numerical examples in what follows. Of course, the immediate idea here is to decrease the time step to make the explicit Euler scheme stable for the Bateman counterpart. However one has to realize that an increase in ε would imply smaller and

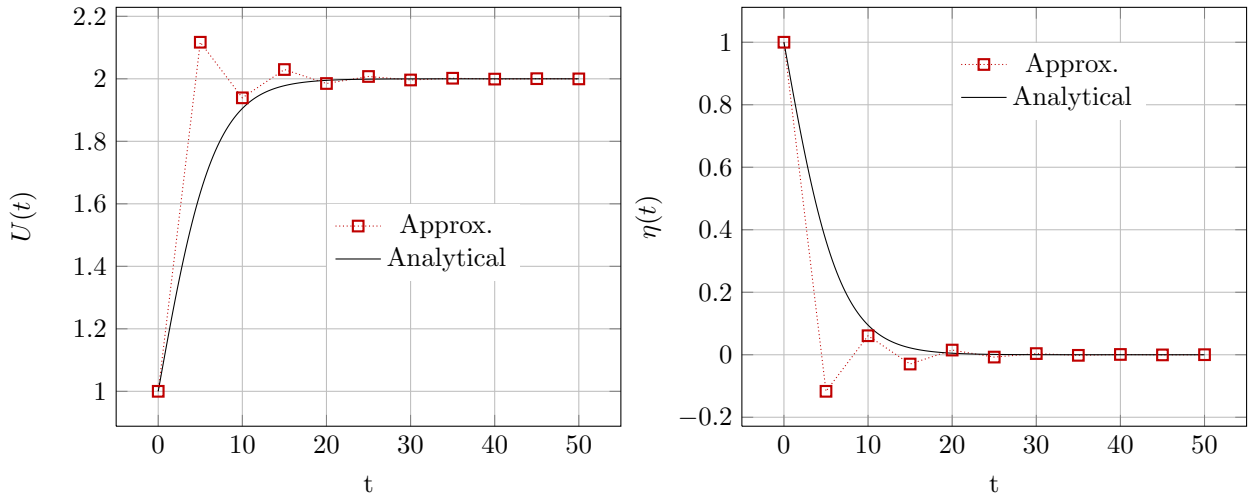

Fig. 2. Analytical solution and computed solution with the non-analog MC scheme/explicit Euler scheme with $N_{MC} = 1000$, $\Delta t = 5$.

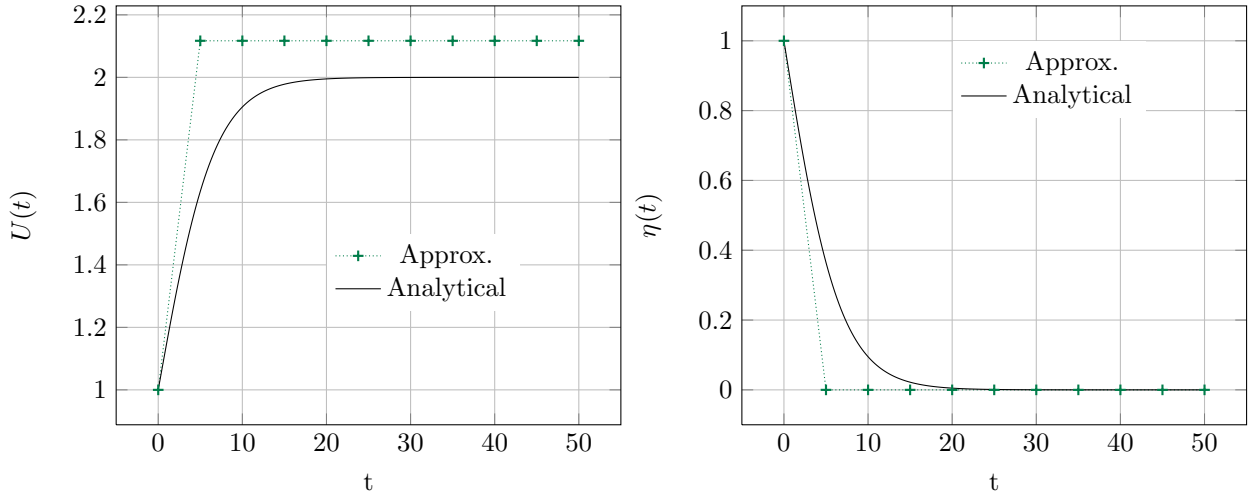

Fig. 3. Analytical solution (black line) and computed solution (green x) with the non-analog MC scheme/explicit Euler scheme with $N_{MC} = 1000$, $\Delta t = 5$ but here we enforce $\eta = 0$ if the time discretization scheme leads to $\eta < 0$.

smaller time-steps and the problem would be postponed rather than solved. In many physical applications, such small time-steps are not computationally affordable, see for example [14, 8] in which long term (late time) simulations are needed. In consequence, we propose analyzing some commonly used alternative schemes.

2.4. *A simple fix-up for the split MC/explicit Euler scheme, application to problem* $1g1r_{\varepsilon=0.15}$-h

Several strategies can be applied in order to avoid the non physical values of the matter density ($\eta < 0$ negative) and, in this case, the presence of oscillations. For example, one can artificially force $\eta = 0$ as soon as $\eta < 0$. This leads to a stable scheme as the state $\eta = 0$ is a stable state of our simplified Bateman counterpart: in fact, in this case, it corresponds to an enforcement of matter density η to its steady-state value. Such fix-up is widely used [14, 13] in the literature.

In fig. 3, we display the results obtained with the split MC/fixed-up explicit Euler scheme in exactly the same conditions as in fig. 2 on problem $1g1r_{\varepsilon=0.15} - h$.

As expected, the fix-up is activated at the first time step and η is enforced to zero, its steady-state value. Solution then preserves the physical property of positiveness of η and does not exhibit an oscillatory behavior. Nonetheless, as we can see in fig. 3 the stationary state for U is now mis-evaluated and the unstationary phase is missed for both observables $U(t)$ and $\eta(t)$. Once again, smaller time step would solve the accuracy problem but many physical problem would lead to unfordable ones.

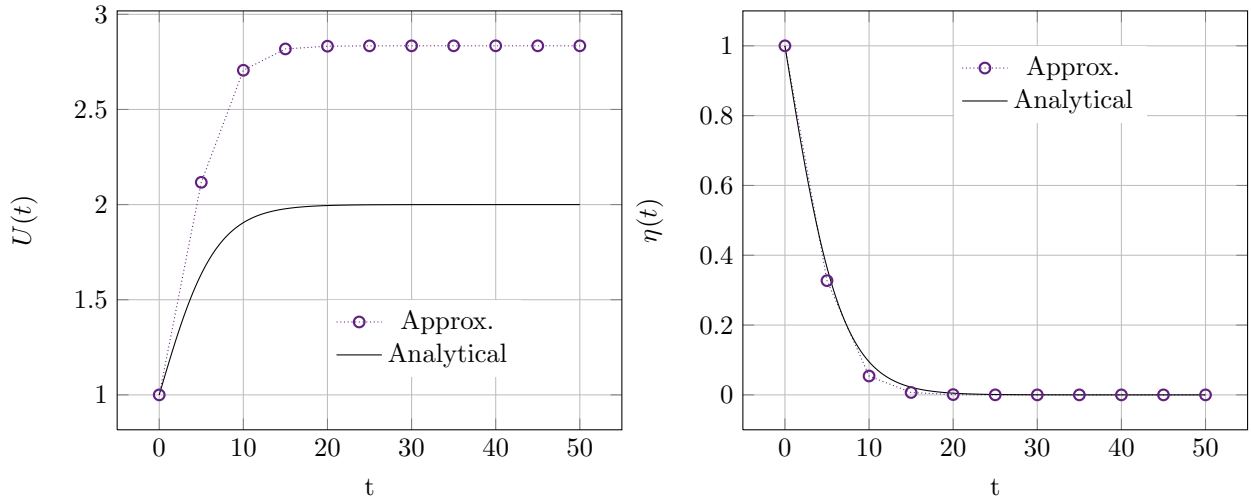

Fig. 4. Analytical solution and computed solution with the non-analog MC scheme/explicit exponential scheme with $N_{MC} = 1000$, $\Delta t = 5$.

2.5. *Split MC/Exponential scheme for the resolution of the Bateman counterpart, application to problem 1g1r$_{\varepsilon=0.15}$-h*

The next method is also widely used in the literature [24]. It ensures by construction the respect of the positivity of matter density for arbitrary time steps Δt. On our simplified problem (2) it consists in writing the Bateman counterpart (2b) as an exponential:

$$\eta(x, \Delta t) = \eta_0(x) e^{\Delta t v \sigma_R^m \int_0^{\Delta t} \int u(s,x,\omega)\, \mathrm{d}\omega\, \mathrm{d}s}.$$

The main difficulty of the exponential method consists in computing accurately the exponential of a matrix, see [17] for 19 ways to do so. Our simplified problem (2) being scalar with respect to the Bateman counterpart (2b), it allows avoiding such numerical difficulty in this study and focusing on the schemes.

Fig. 4 presents the results obtained in the same conditions as in figures 2 and 3 of pages 5 and 5 but with the split MC/exponential method with explicit density applied to our simplified problem 1g1r$_{\varepsilon=0.15}$-h. First, fig. 4 shows that the scheme ensures the positivity of the matter density. The time evolution of η is non oscillatory and the approximation for η is clearly better than on fig. 3 on the preceding page: the steady state for η is here recovered without enforcing it. However, the increasing accuracy on η clearly does not ensure better accuracy on U and the particle density steady-state is once again mis-evaluated. In fact, on this problem, the accuracy of the split MC/exponential scheme for U (fig. 4) is even worse than the accuracy of the split MC/explicit Euler scheme with enforced steady-state (fig. 3 on the preceding page). This is emphasized in the numerical convergence studies of figure fig. 5 on the next page. As the exponential method in more expensive (in particular, the non-scalar case needs the estimation of the exponential of a matrix), we tend to prefer the split MC/fixed-up explicit Euler scheme. The latter will be used as a reference in the next sections, especially when analytical solutions are not available.

2.6. *Convergence studies for the different schemes on problem 1g1r$_{\varepsilon=0.15}$-h-Δx*

In this section, we deepen the above qualitative studies by performing quantitative numerical convergence ones with respect to the two approximation parameters, N_{MC} and Δt. Note that such studies are possible only because we have an analytical solution for the simplified problem in the uniform case. Our aim here is to emphasize an accuracy issue common for the three above schemes, and indeed all schemes based on a splitting between the transport phase and the Bateman one.

Fig. 5 on the following page presents convergence studies with respect to N_{MC} for $\Delta t \in \{5.0, 5.0 \times 10^{-2}, 5.0 \times 10^{-4}\}$ with N_{MC} going from 2^1 to 2^{17} each step multiplying by 2. In a log-log plot, each point is the mean of absolute errors on $U(t)$ in L_1 norm at $N_t = 11$ checkpoints/times of interest (the same as in figures 2, 3 and 4 of pages 5, 5 and 6) for $N_s = 128$ launches with different seeds. Each point in fig. 5 on the next page with discretization parameters $\Delta t, N_{MC}^s$ is then computed thanks to the following expression (where the dependence with respect to the seed s is explicit on N_{MC}^s):

$$e_{\Delta t, N_{MC}} = \frac{1}{N_t} \sum_{l=1}^{N_t=11} \left[\frac{1}{N_s} \sum_{s=1}^{N_s=128} |U_{analytic}(t_l) - U_{\Delta t, N_{MC}^s}(t_l)| \right]. \tag{6}$$

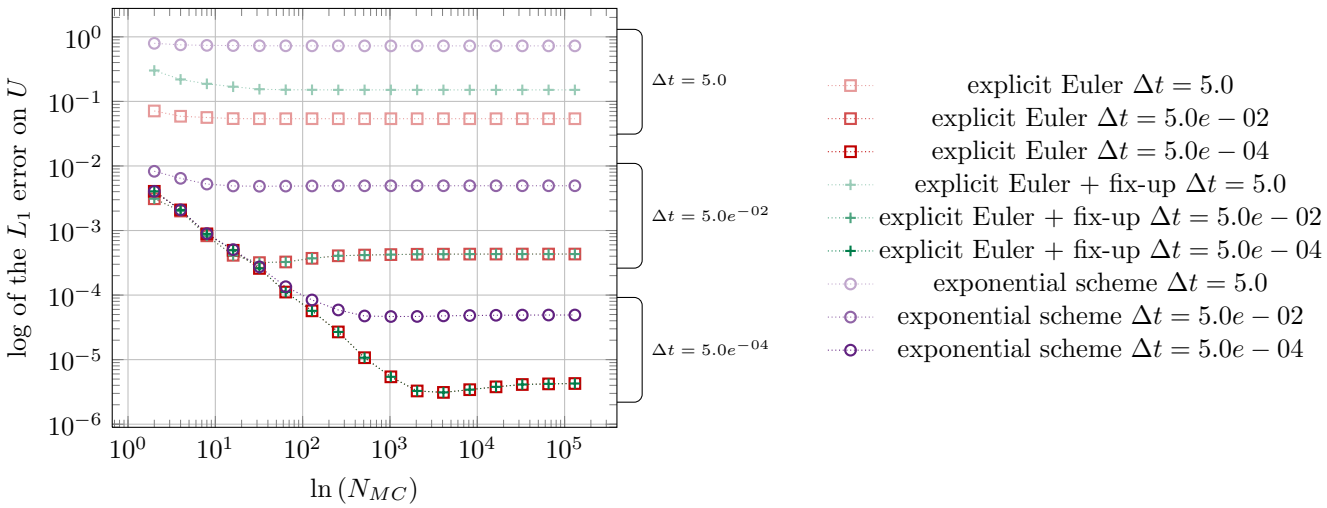

Fig. 5. Convergence study for the three presented schemes of the section with $\Delta t = 5.0e^{+00}, 5.0e^{-02}, 5.0e^{-04}$ and $N_{MC} = 2, 4, 8, ..., 131072$.

The MC scheme for these convergence studies is the non-analog one described in appendix A.3. The simulation domain has two cells and we remind the reader that the solution is homogeneous: the capability of the MC method to preserve the homogeneous state is here tested as the two cells do not have exactly the same MC statistics. In fact, there is a different level of accuracy between both cells depending on their respective number of particles, this number changing dynamically during the simulation). The configuration denotation 1g1r$_\varepsilon$-h is suffixed by Δx in the following.

Let us first comment the first three curves obtained with $\Delta t = 5$: the main result is that the performances of the three split schemes are independent of the MC discretization. The MC error is overwhelmed by the time discretization error (i.e. $\mathcal{O}(\Delta t)$). Also, as observed in the previous sections, the split MC/exponential scheme is poorer than the fixed-up explicit Euler one which is poorer than the explicit Euler one (even if oscillatory and not physical).

This is confirmed by the three curves for the three schemes with $\Delta t = 5.0 \times 10^{-2}$. First the time-step is small enough so that the fix-up is not activated and the split MC/fixed-up explicit Euler scheme degenerates toward the split MC/explicit Euler scheme. Second, once again $\forall N_{MC}$, the accuracy of the split MC/exponential scheme is poorer than the accuracy of the split MC/explicit Euler one. Finally, we observe a change in the slopes of the curves occurring between $N_{MC} = 10$ and $N_{MC} = 100$: this corresponds to a change of regime of the numerical approximation. Indeed convergence first depends on the number of particles N_{MC} (the error being lead by the MC scheme) and once enough particles are used, the error stagnates to $\mathcal{O}(\Delta t)$ because we enter the time discretization regime.

This phenomenon is also confirmed by the last three curves for the three schemes with $\Delta t = 5. \times 10^{-4}$ for which the N_{MC} dependent regime is maintained until about 2000 particles (with explicit Euler) before stagnating to an accuracy dictated by the time discretization $\mathcal{O}(\Delta t)$ of the Bateman counterpart of problem (2). It is worth noting that the accuracy reached by schemes at $\Delta t = 5. \times 10^{-4}$ is exactly two decades better than with $\Delta t = 5. \times 10^{-2}$ which is coherent.

Consequently, although stability and physical properties can be problematic, we insist on the fact that the three schemes presented so far converge as long as one can afford increasing numbers of particles and decreasing time-steps, depending on the regime. This conclusion justifies the use of such schemes as reference, in following sections, when no analytical solution is available. However, note that time-steps necessary to ensure *stability* or *respect of physical properties (positiveness etc.)* can be prohibitive on a true physical problem [14, 8, 7].

Our main point here is to emphasize that even if one can afford time-steps such that *stability and/or respect of physical properties* is ensured, this does not guarantee an accurate approximation. Lastly, we overall put forward another important aspect which is scarcely tackled in the literature to our knowledge: consider fig. 5 and the curves for $\Delta t = 5.0 \times 10^{-2}$, when one chooses $N_{MC} > 32$, computational time is lost as an approximation with one million MC particles will have the same accuracy as an approximation with only one hundred. Such assessment of waste of computational resources was also tackled in [6].

2.7. *Few words on adaptive time-steps, predictor-corrector schemes, implicit schemes etc.*

The above schemes for time discretization are very simple and are not necessarily the standard in simulation codes for the coupling of transport equation with Bateman system. Nonetheless, more elaborate schemes present the same drawbacks as seen in [5, 13, 8, 7].

For example, more or less complex predictor-corrector schemes can be applied but several papers show that they still

lack stability when some materials have stiff reaction rate with respect to the scales at stake, see [8]. Otherwise, simple schemes with adaptive time-steps would inevitably lead to unfordable ones.

In [8], the authors explicitly claim the need for *a new stable method*. They even suggest one in [7], a *stochastic implicit Euler* scheme ensuring stability for arbitrary time steps. To our knowledge, this scheme is the most advanced one for the coupling of transport equation *with a MC resolution* with Bateman equations. It can be applied reusing the classical architecture for the coupling (alternating between a simulation code for the transport equation and another one for the Bateman system), it is stable and prevents from obtaining non physical quantities. Besides, it allows dealing with time discretization *together with* geometrical effects. However, the scheme is computationally intensive: in brief, it needs the resolution of a non linear stochastic root-finding problem together with robust stopping criterion for the iterative scheme. Note that some authors (non exhaustive list) [20, 22, 21] suggest methods with comparable efficiency with respect to stability and preservation of physical quantities for coupling transport equation to other physics but rely on a multigroup diffusion solver for the transport equation which is beyond the scope of this paper. Finally, in our opinion the main drawback of this scheme (shared with the other ones) comes from its accuracy in $\mathcal{O}(\Delta t)$ potentially limiting affordable precision and prone to waste of computational resources as emphasized in section 2.6 on page 6.

2.8. *Summary of this section*

The combination of MC scheme for transport with time discretization schemes for Bateman system can lead to
(i) numerical instabilities (spurious oscillatory behavior),
(ii) non physical behaviors (negative matter density η),
(iii) waste of computational resources (see the example of section 2.6 on page 6).
It is worth noting that these points would have also been observed with the semi-analog scheme of appendix A.2 for the MC phase. In other words, the results are independent of the schemes at use in the different phases.

In the following, we suggest an original alternative to the existing methods: it consists in dropping the common trait of all those schemes, i.e. the use of a splitting scheme between transport equation and Bateman system. To do so we will introduce a new MC scheme and present in which ways it allows improving the three above points (i)–(ii)–(iii).

3. A new unsplit scheme for the resolution of the *simplified* coupled problem

When splitting transport and Bateman phases, the main hypothesis consist in freezing the matter density during transport, and solve its evolution in the second phase. Our aim is to alleviate this hypothesis. To do so, we need two ingredients :
- If matter density isn't constant during a time step, we need a Monte-Carlo scheme with non-constant characteristics.
- As we don't know the exact evolution of matter density over a time step, we need a way to approach it.

The mathematical legitimacy of such time dependent characteristics MC method is not new and we mainly refer to [19]. The existence of such Monte-Carlo method widen the sphere of possibilities. In a first time we choose to use the analytical solution established in section 2.1 on page 3 as it is available here. The main idea is to consider each cell as a local uniform problem (for which the analytical solution is known) to estimate matter density evolution rather than freezing it. We will then apply the freshly built scheme to the test problems of section 2.2 on page 4 and experimentally verify its properties (points (i)–(ii)–(iii) of section 2.8).

3.1. *Time discretization for the MC solved transport equation for the simplified coupled problem*

As detailed in [19], solving the transport equation with time/space dependent characteristics is possible. Let us consider the transport equation (A.1) but with time dependent characteristics (we will explicit the dependences with respect to the Bateman evolution when necessary):

$$\partial_t u(x,t,\omega) + v\omega\nabla u(x,t,\omega) + v\sigma_t(t)u(x,t,\omega) = \int v\sigma_s(t)P_s(t,\omega,\omega')u(x,t,\omega')\,\mathrm{d}\omega'. \tag{7}$$

The idea is once again to rewrite (7) in an integral form and to introduce the relevant random variables so that the equation can be rewritten as an expectation over these ones. All calculations completed, we obtain

$$u(x,t,\omega) = \mathbb{E}\left[u_0(x-v\omega t,\omega)e^{-\int_0^t v\sigma_a(\alpha)\,\mathrm{d}\alpha}\mathbf{1}_{[t,\infty[}(\mathcal{S}) + u(x-v\omega\mathcal{S},t-\mathcal{S},W')e^{-\int_{t-\mathcal{S}}^t v\sigma_a(\alpha)\,\mathrm{d}\alpha}\mathbf{1}_{[0,t]}(\mathcal{S})\right], \tag{8}$$

where $W' \sim P_s(t-\mathcal{S},\omega,\omega)$ the angular scattering law and $\mathcal{S} \sim \mathcal{E}_t(v\sigma_s)$ the time scattering law where $\mathcal{E}_t(v\sigma_s)$ denotes the probability law of the random variable having for pdf

$$f(s) = \mathbf{1}_{[0,\infty]}(s) v\sigma_s(t-s) e^{-\int_{t-s}^{t} v\sigma_s(\alpha)\,\mathrm{d}\alpha}.$$

By a change of variable in the exponential ($t-\beta=\alpha$), we get

$$f(s) = \mathbf{1}_{[0,\infty]}(s) v\sigma_s(t-s) e^{-\int_{0}^{s} v\sigma_s(t-\beta)\,\mathrm{d}\beta}.$$

The cumulative density function is given by:

$$F(s) = \int_{-\infty}^{s} f(s)\,\mathrm{d}s = 1 - e^{-\int_{0}^{s} v\sigma_s(t-\beta)\,\mathrm{d}\beta}.$$

Given the fact that

$$\int_{t}^{\infty} f(s)\,\mathrm{d}s = e^{-\int_{0}^{t} v\sigma_s(t-\beta)\,\mathrm{d}\beta},$$

it is simple verifying the pdf weights to 1.

The previous laws are expressed in an adjoint form whatever the dependence of the characteristics with respect to time, we rely to [19] in order to express them in a direct form. We will refer to $\mathcal{E}_t(v\sigma_s)$ as an exponential law as in [19], extending it to non constant parameters.

We are now interested in the above samplings in the case the characteristics evolve with respect to Bateman equation, more precisely, in this section, according to (5).

3.2. *Choice of the time evolution of the material density $\eta(t)$*

The main idea is to approach matter density evolution considering each cell as a local uniform problem, so that we have an analytical expression for $\sigma_\alpha(t) = \sigma_\alpha^m \eta(t)$ given in (5). For the sake of pedagogy, the mathematical justification of such a choice is postponed to section 5 on page 21 in which the complete methodology is detailed. Let us now describe how this choice affect the MC scheme steps:

– **Sampling of the interaction time** In order to sample a random variable $\mathcal{S}$ whose pdf is given by f, a common method consists in inversing the associated cdf F. This allows sampling from a uniform law $\mathcal{U}$ on $[0,1]$ before applying a transformation F^{-1}: in other words, $\mathcal{S} = F^{-1}(\mathcal{U})$. The cdf of the interaction time is given by

$$F(\gamma) = \int_{-\infty}^{\gamma} f(s)\,\mathrm{d}s = 1 - e^{-\int_{0}^{\gamma} v\sigma_s(t-\beta)\,\mathrm{d}\beta}.$$

In order to sample from a uniform law, we need to inverse the cdf of the law

$$\mathcal{U} = \int_{-\infty}^{\mathcal{S}} f(s)\,\mathrm{d}s = 1 - e^{-\int_{0}^{\mathcal{S}} v\sigma_s(t-\beta)\,\mathrm{d}\beta}.$$

Now, plugging the expression of $\sigma_s(t) = \sigma_s^m \eta(t)$ in the formula above we get (we dropped the exponents ^{m} for conciseness)

$$\sigma_s(t) = \sigma_s \eta(t) = \sigma_s \frac{(\sigma_R U_0 + \eta_0 \sigma_a)\eta_0}{\sigma_R U_0 e^{-v(\sigma_R U_0 + \eta_0\sigma_a)t} + \eta_0 \sigma_a}.$$

After few calculations one gets:

$$\mathcal{S} = t - \frac{1}{v(\sigma_a\eta_0 + U_0\sigma_R)} \ln\left(\frac{(\eta_0\sigma_a e^{vt(\sigma_a\eta_0 + U_0\sigma_R)} + \sigma_R U_0) e^{\frac{\sigma_a}{\sigma_s}\ln(\mathcal{U})} - \sigma_R U_0}{\eta_0 \sigma_a} \right).$$

We can verify that at the first order with respect to $\sigma_R \sim 0$ we have $\mathcal{S} \underset{\sigma_R\sim 0}{=} -\frac{1}{v\sigma_s\rho_0}\ln(\mathcal{U})$ which corresponds to the sampling of the interaction time when considering constant characteristics. We can even put forward the second order development with respect to σ_R we get

$$\mathcal{S} \underset{\sigma_R\sim 0}{=} -\frac{1}{v\sigma_s\eta_0}\ln(\mathcal{U}) + \left(\frac{U_0 t}{\sigma_a\eta_0} + \frac{U_0(1-\mathcal{U}^{\frac{\sigma_a}{\sigma_s}})}{v\sigma_a^2\eta_0^2 e^{v\sigma_a\eta_0 t}} - \frac{U_0\left(v\sigma_a\eta_0 t - \frac{\ln(\mathcal{U})\sigma_a}{\sigma_s}\right)}{v\sigma_a^2\eta_0^2} \right)\sigma_R + \mathcal{O}(\sigma_R^2). \tag{9}$$

Higher order approximations can be obtained in the same manner.

– **Particle weight modifications**: Similarly, we use the analytical time evolution of η in order to approximate the weight modification of the particles along their flight path. We have

$$\sigma_a(t) = \sigma_a \eta(t) = \frac{\eta_0 \sigma_a e^{(\sigma_R U_0 + \eta_0 \sigma_a) v t}}{1 + \frac{\eta_0 \sigma_a}{\sigma_R U_0 + \eta_0 \sigma_a} \left(e^{(\sigma_R U_0 + \eta_0 \sigma_a) v t} - 1 \right)},$$

so that,

$$\int_{t-s}^{t} \sigma_a(\alpha)\, \mathrm{d}\alpha = \frac{1}{v} \ln \left(\frac{U_0 \sigma_R + \sigma_a \eta_0 e^{((\sigma_a \eta_0 + U_0 \sigma_R) v t)}}{U_0 \sigma_R + \sigma_a \eta_0 e^{(\sigma_a \eta_0 + U_0 \sigma_R) v (t-s))}} \right)$$

and finally we get for the weight modification along the flight path

$$e^{-v \int_{t-s}^{t} \sigma_a(\alpha)\, \mathrm{d}\alpha} = e^{-\ln \left(\frac{U_0 \sigma_R + \sigma_a \eta_0 e^{(\sigma_a \eta_0 + U_0 \sigma_R) v t}}{U_0 \sigma_R + \sigma_a \eta_0 e^{(\sigma_a \eta_0 + U_0 \sigma_R) v (t-s))}} \right)} = \frac{U_0 \sigma_R + \sigma_a \eta_0 e^{(\sigma_a \eta_0 + U_0 \sigma_R) v (t-s))}}{U_0 \sigma_R + \sigma_a \eta_0 e^{(\sigma_a \eta_0 + U_0 \sigma_R) v t}} = \frac{U(t)}{U(t-s)} \quad (10)$$

Of course, if $v \sigma_a \eta(t) = cst$ we degenerate to the classical particle weight modification $e^{-v \sigma_a \eta_0 s}$ along the flight path (appendix A.3) and once again, higher order approximations with respect to $\sigma_R \sim 0$ can be obtained (not presented here due to their complex forms).

– **Sampling the scattering angle**: On our simplified problem, we considered an isotropic scattering angle in order to avoid additional difficulties. We will explain how to modify the sampling of the direction in the very general case in section 5 on page 21.

– **Treatment when crossing a discontinuity**: At this stage, we may describe how we proceed when a MC particle crosses the boundary between two cells. In order to avoid repetitions, we present a general study of this treatement in section B on page 34.

Let us now revisit the previous stiff test-problem of section 2.2 on page 4 with the above described Unsplit Time-Dependent Monte-Carlo (UMC) scheme.

3.3. *Stiff reaction rate test problem with the new UMC scheme, application to problem 1g1r$_\varepsilon$-h*

In this section we begin applying the UMC scheme to the problem 1g1r$_\varepsilon$-h considering the same observables as in section 2 on page 3, namely $U(t), \eta(t)$. Then, we will present some deepened convergence studies on problem 1g1r$_\varepsilon$-h-Δx on those same quantities for which we have analytical solutions at hand. Finally, we will change the test-case for 1g1r$_\varepsilon$-nh (nh for non-homogeneous), and compare results of classical split scheme and the UMC scheme. As we do not have analytical solutions for 1g1r$_\varepsilon$-nh, we will rely on very fine resolution of the classical split scheme as reference. We aim at experimentally showing that the UMC scheme improves the points (i)–(ii)–(iii) of section 2.8 on page 8.

Fig. 6 on the following page presents the time evolution of $U(t), \eta(t)$ obtained with the UMC scheme on the stiff problem 1g1r$_{\varepsilon=0.15}$-h of section 2.2 on page 4. On such observable and configuration, the UMC scheme allows recovering the analytical solution up to machine accuracy for any time-step *with only one MC particle as there is only one cell*: in this sense, we consider the UMC scheme takes into account the points (i)–(ii) of section 2.8 on page 8 regarding stability.

Furthermore, we consider the UMC scheme extends the property of the non-analog MC scheme to cases where time evolution of the characteristics is known in the sense that it is natively analytical [2] in this case (while non-analog scheme of appendix A.3 is analytical on uniform problems when matter properties are constant).

This property is emphasized on left graphic of fig. 7 on the following page in which a convergence study with respect to Δt is performed for the split schemes of section 2 on page 3 and for the UMC scheme of section 3 on page 8 with only 1 MC particle for transport phase and only one cell, i.e. problem 1g1r$_{\varepsilon=0.15}$-h. On this figure, we can see that the split schemes have an $\mathcal{O}(\Delta t)$ accuracy whereas the UMC scheme ensures an accuracy below 10^{-11} (roundoff errors). Here again, each point is computed in the same condition as in section 2.6 on page 6 with respect to expression (6).

Now, as in the previous section, we consider more than 1 cell but still on the same homogeneous test-problem described in table 1 on page 4, i.e. problem 1g1r$_{\varepsilon=0.15}$-h-Δx. The results obtained with 2 cells and 128 MC particles are presented in the right graphic of fig. 7 on the next page. The scales are identical so that we can appreciate the difference.

As expected, with 2 cells, the UMC approach is not analytical anymore as a space discretization breaks homogeneity (the MC statistics is not exactly the same in each cell). Nevertheless, the convergence study with respect to Δt of the right graphic of fig. 7 on the following page allows emphasizing the UMC approach is less sensitive to time discretization than the split ones : indeed, with large Δt, the accuracy is time-step dependent and error decreases linearly with Δt

[2] Precisely, we want to highlight here a class of Monte-Carlo schemes delivering the exact solution on integrated observables in specific situations. Here, the problem being homogeneous, using analytical solution of $\eta(t)$ on transport characteristics leads to exact results.

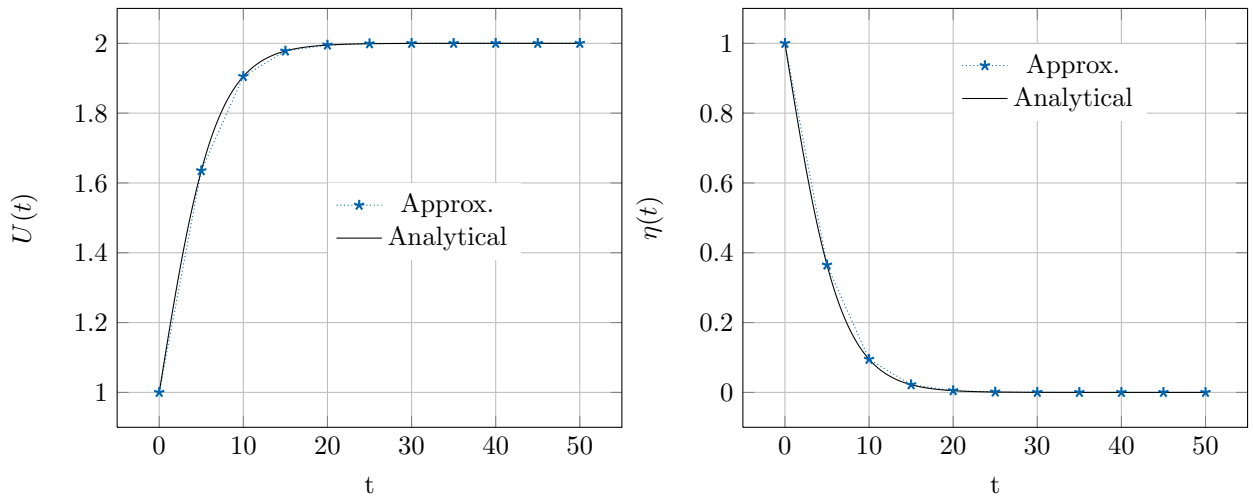

Fig. 6. Analytical solution and computed solution with our new MC scheme with $N_{MC} = 1000$, $\Delta t = 5$ (same conditions as in section 2.2 on page 4).

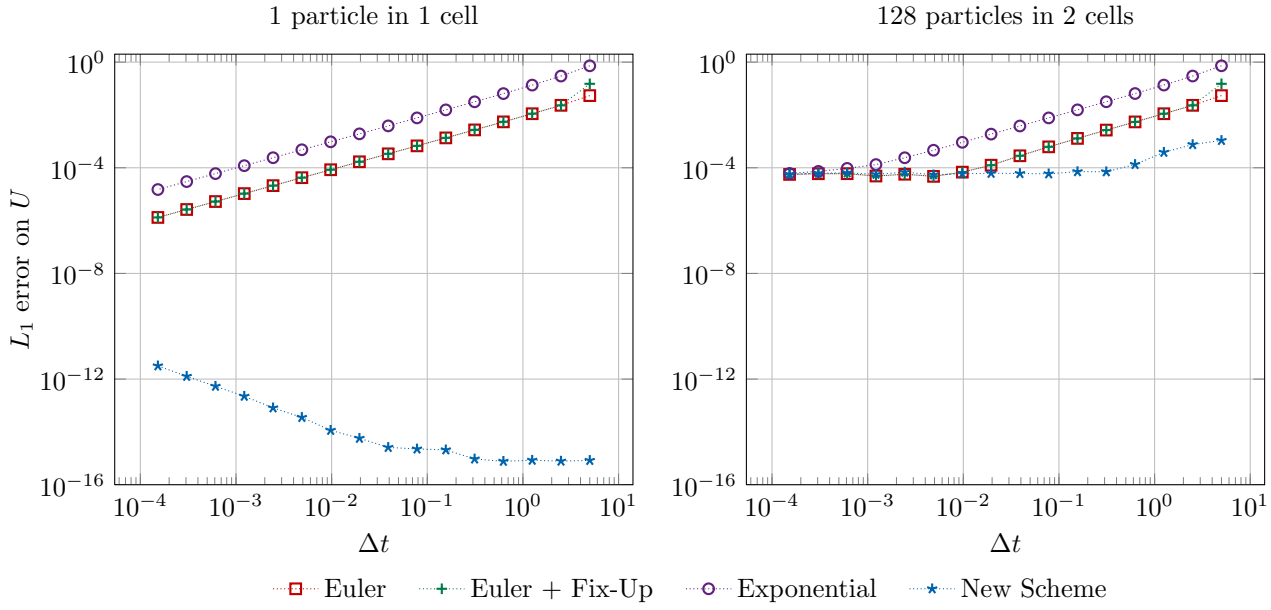

Fig. 7. Comparison of convergence of the UMC scheme with the splitted schemes of previoux section. Pb 1, left : (1 cell, 1 Monte-Carlo particles) / right : (2 cells, 1024 Monte-Carlo particles)

for the split methods ($\mathcal{O}(\Delta t)$ regimes). Once Δt is small enough, the accuracy becomes N_{MC}-dependent, and we reach a floor, asymptotically with Δt, common for every approaches as the same number of MC particles is used for each schemes. Finally, with this example, we insist on the fact we built a new MC scheme rather than suggesting a variance reduction procedure. Indeed, the UMC scheme does not reduce variance: on the second graphic of fig. 7, for $\Delta t < 10^{-2}$ both the classical and the new one have the same error. It only allows the accuracy to be more rapidly reached regarding time discretization.

Fig. 8 on the following page presents some convergence studies with respect to N_{MC} for 2 different time discretizations ($\Delta t = 5.0e^{-02}$ and $\Delta t = 5.0e^{-04}$) on the problem 1g1r$_{\varepsilon=0.15}$-h-Δx (table 1 on page 4) which we remind has 2 cells (in order not to be analytical with the new UMC non-analog scheme). With the split schemes, as N_{MC} increases, the slopes of the convergence curves stagnate at a floor which is closely related to the time discretization ($\mathcal{O}(\Delta t)$) whereas with the UMC scheme the accuracy is independent of the time discretization, on this test problem. In this sense, we think the UMC scheme avoids a waste in computational resources (point (iii) of section 2.8 on page 8). Indeed, for the split fixed-up Euler scheme for example once time-step is set to $\Delta t = 1.28 \times 10^{-2}$, choosing $N_{MC} = 32$ or $N_{MC} = 131072$ allows the same accuracy. Of course, decreasing the time step allows postponing the problem but still, with $\Delta t = 5.0e^{-04}$, the accuracy of the explicit Euler scheme is the same between $N_{MC} = 2048$ and $N_{MC} = 131072$ particles.

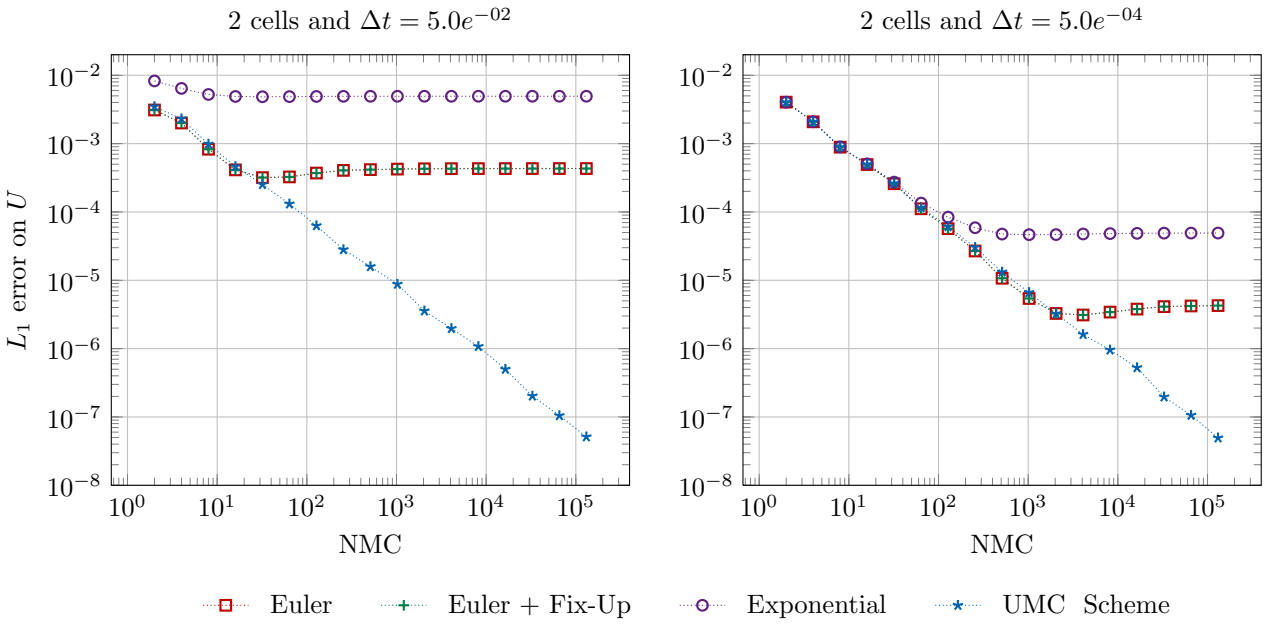

Fig. 8. Comparison of convergence of the UMC scheme with the splitted schemes of previoux section. Pb 1, 2 cells, left : $\Delta t = 5.0e^{-02}$ / right : $\Delta t = 5.0e^{-04}$

3.4. *Non homogeneous Spatial test problem 1g1r$_{\varepsilon=0.45}$-nh (not analytical)*

Let us now modify slightly the test problem of section 2.2 on page 4: we take the same configuration but we set $\varepsilon = 0.45$ (stiffer test problem) and apply some 'vacuum' boundary conditions on the right hand side of a 1 dimensional slab geometry, the problem will be denoted by 1g1r$_{\varepsilon=0.45}$-nh.

U_0	η_0	v	σ_t^m	σ_s^m	σ_R^m	ε	left BC	right BC
1.00	1.00	1.00	1.00	$1+\varepsilon$	$-\varepsilon$	0.45	specular	free

Fig. 9. Parameters for the test problem 1g1r$_{\varepsilon=0.45}$-nh.

The problem is not anymore homogeneous and no analytical solution is available to our knowledge. In the following, the *classical* scheme will stand for a split scheme between the transport and the matter evolution, with the MC scheme of appendix A.3 in order to solve the Transport phase, and the fixed-up explicit Euler scheme for the Bateman phase. As reference for our comparisons, we rely on a finely discretized configuration of the split scheme of section 2.4 on page 5.

Let us denote by $\mathcal{D}$ the simulation domain, here $\mathcal{D} = [0, 1]$. Fig. 10 on the next page presents the time evolutions of particle and material density, $U(t) = \frac{1}{|\mathcal{D}|}\int_{\mathcal{D}}\int u(x,t,\omega)\,\mathrm{d}\omega\,\mathrm{d}x$ and $\eta(t) = \frac{1}{|\mathcal{D}|}\int_{\mathcal{D}}\eta(x,t)\,\mathrm{d}x$, for the classical scheme and the UMC scheme we describe in section 3 on page 8. With the classical scheme, the resolution scheme needs a time step $\Delta t \approx 0.128$ to be considered converged for a variation of less than 1% on $U(t), \eta(t)$ for the eleven measurement times whereas we reach this accuracy with $\Delta t = 0.8192$ using the UMC scheme.

We suggest presenting some results on spatial profiles at time $t = 1.6384$ for the particle density $U(x,t) = \int u(x,t,\omega)\,\mathrm{d}\omega$ and the material density $\eta(x,t)$. The results are displayed in fig. 11 on page 14 with 100 cells, $N_{MC} = 12800$ and several time discretizations. On the same figure, they are compared to the computed reference results using $\Delta t = 1.0e^{-04}$ and more than 1.6 billion particles obtained with the classical scheme. In these conditions, this leads to very smooth spatial results. Note that such accuracy (with respect to the MC discretization mainly) has been possible thanks to the parallel replication ability of our simulation code [9].

The top pictures of fig. 11 on page 14 present the spatial profiles of particle density at $t = 1.6384$ for the classical scheme and the UMC scheme for several time discretizations but the same MC discretization $N_{MC} = 12800$: on such observable, we can identify a lack of resolution only for the coarser time discretization $\Delta t = 1.6384$ with the split scheme, but it becomes really unclear for smaller time steps. Differences on this observable could be noticed but a very accurate MC resolution would be needed and only then we would realize a finer time discretization is needed (an illustration of this is given in fig. 12 on page 15). However, when considering the matter density spatial profiles plotted on bottom pictures of fig. 11 on page 14 with common scales, in the same conditions, we experience important differences between

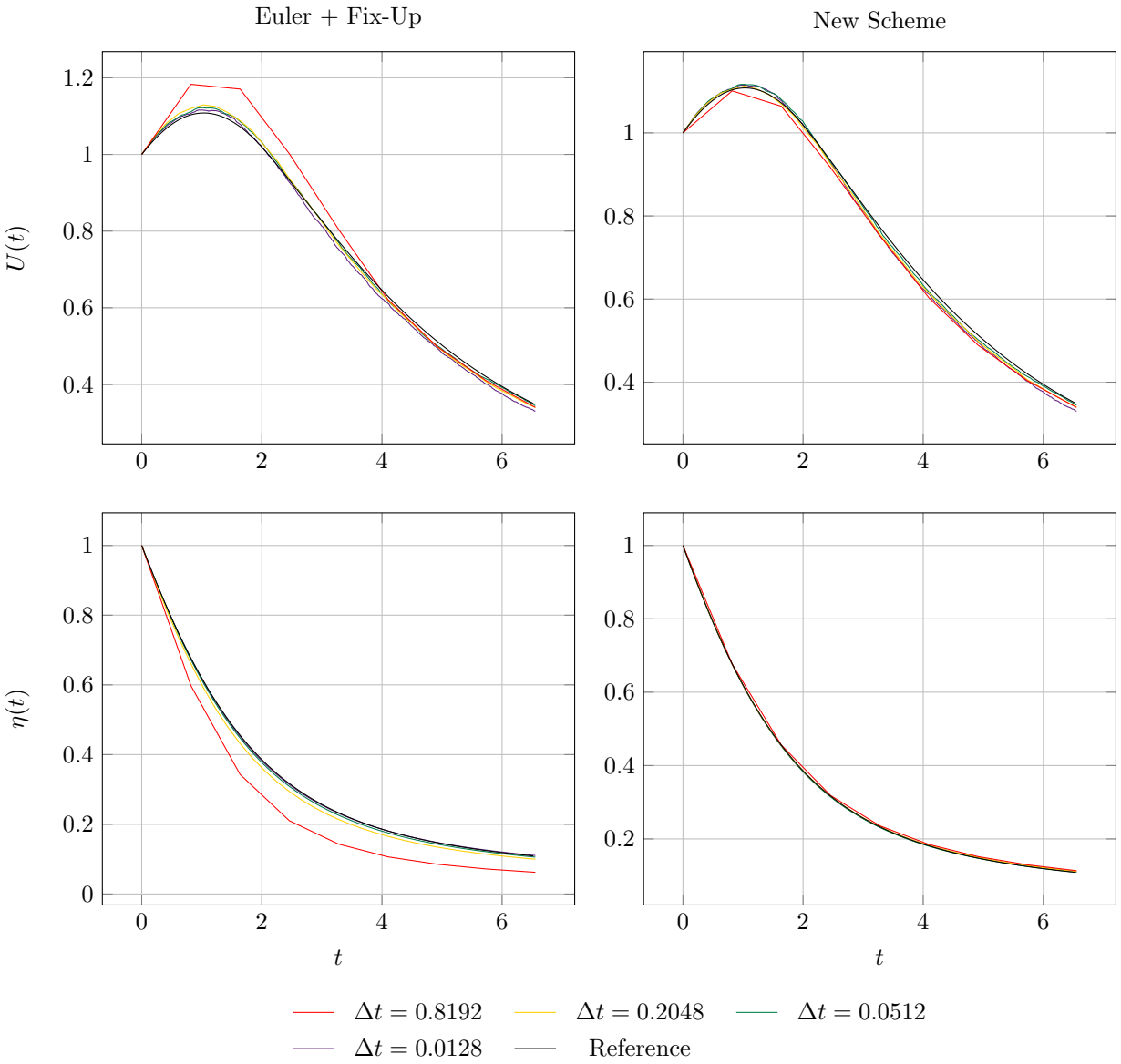

Fig. 10. Time evolution of $U(t)$ and $\eta(t)$ for the configuration of section section 2.2 on page 4 with $\varepsilon = 0.45$ for the classical scheme (left) and the new MC scheme (right) for several time discretizations Δt and $N_{MC} = 10000$.

time discretizations: with $\Delta t = 1.6384$, the fix-up is activated from $x = 0$ up to $x = 0.3$ for $t = 1.6384$ and the matter density profile is very far from the one obtained with $\Delta t = 0.128$ which is close to be converged. Let us emphasize the fact that without fix-up, instabilities would appear around $x = 0$ and the spatial profiles would be very oscillating. With the UMC scheme,we observe that the spatial profiles for the material densities are much less sensitive to time discretization (fig. 11 on the next page bottom right). The approximation does not exhibit instabilities (i), does not exhibit non-physical matter density (ii) and is less sensitive to the time discretization (iii), MC ressources in terms of computational time and memory are not wasted.

Fig. 12 on page 15 allows comparing spatial profiles of particle and material density obtained with the 2 schemes with more than 1.6 billion particles for several time discretizations. On one hand, with such MC discretization the lack of accuracy with respect to time discretization of the reference scheme can be identified even on the spatial profiles of the particle density, at the price of prohibitive computational cost (to compare with fig. 11 on the following page where only the number of particle is different). On the other hand, with the UMC approach (right column), the results are almost insensitive to time discretization while converging toward the reference curves. More precisely, on fig. 11 on the next page (top-right), a small discrepancy is noticeable for the largest time-step ($\Delta t = 1.6384$, red curve in top right graph) with respect to the reference curve. This discrepancy could not be observed on the previous homogeneous problems: we postulate spatial effects may still impose a constraint on the time step.

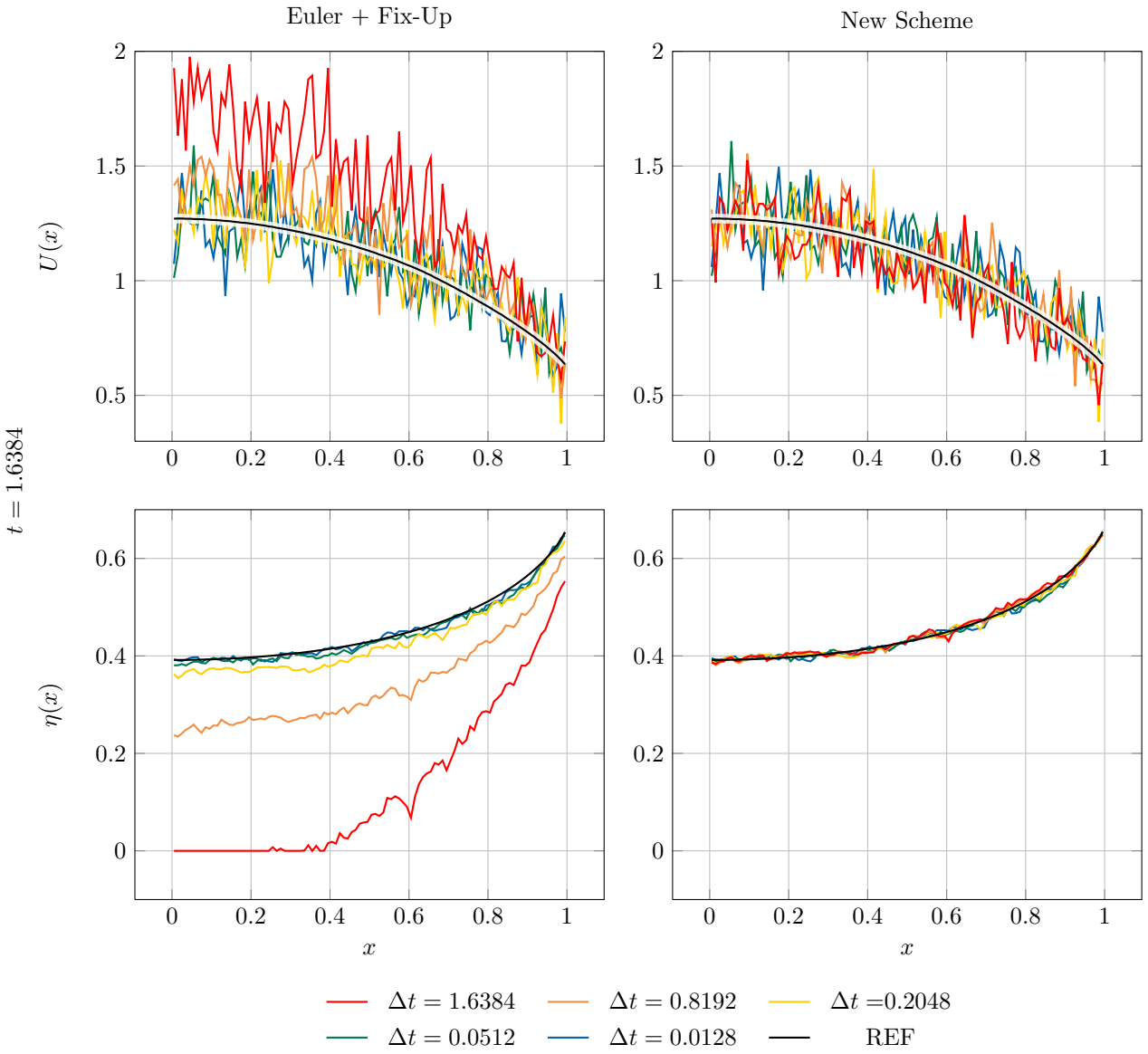

Fig. 11. Spatial profiles for the particle density $U(x, t = 1.6384) = \int u(x, t = 1.6384, \omega)\,\mathrm{d}\omega$ and component density $\eta(x, t = 1.6384)$ at $t = 1.6384$ for the classical scheme (left) and the new MC scheme (right) for $N_{MC} = 12800$ for the configuration problem # 2 (figure table 1 on page 4) for several time discretizations Δt and 100 cells.

4. Monokinetic transport coupled to non degenerate (a.k.a. non-scalar) Bateman system

In the previous section, we presented a new MC solver for the resolution of the coupled transport equation with the Bateman system *in a simplified configuration with 1 group/1 material*. We experimentally presented its numerical properties on a simplified problem (2) and consider the results encouraging enough (with respect to points (i), (ii) and (iii) of section 2.8 on page 8) to work on an extension of the solver to more complex and general ones. The aim of this section is then to progressively relieve the simplifications done in section 2 on page 3 and step-by-step apply the new MC solver to multi-material Bateman system (i.e. non-scalar case) before introducing energy/velocity dependence (non-monokinetic case in section 5 on page 21).

4.1. *Extension to non-scalar Bateman system*

Let us first consider the monokinetic transport equation coupled with the non-scalar Bateman system. For the description of the solver in this section, we mainly need to consider the homogeneous case (independence of the solution with respect to x) so that only remains time dependence (see section 2 on page 3) as the MC pre-treatment of the transport

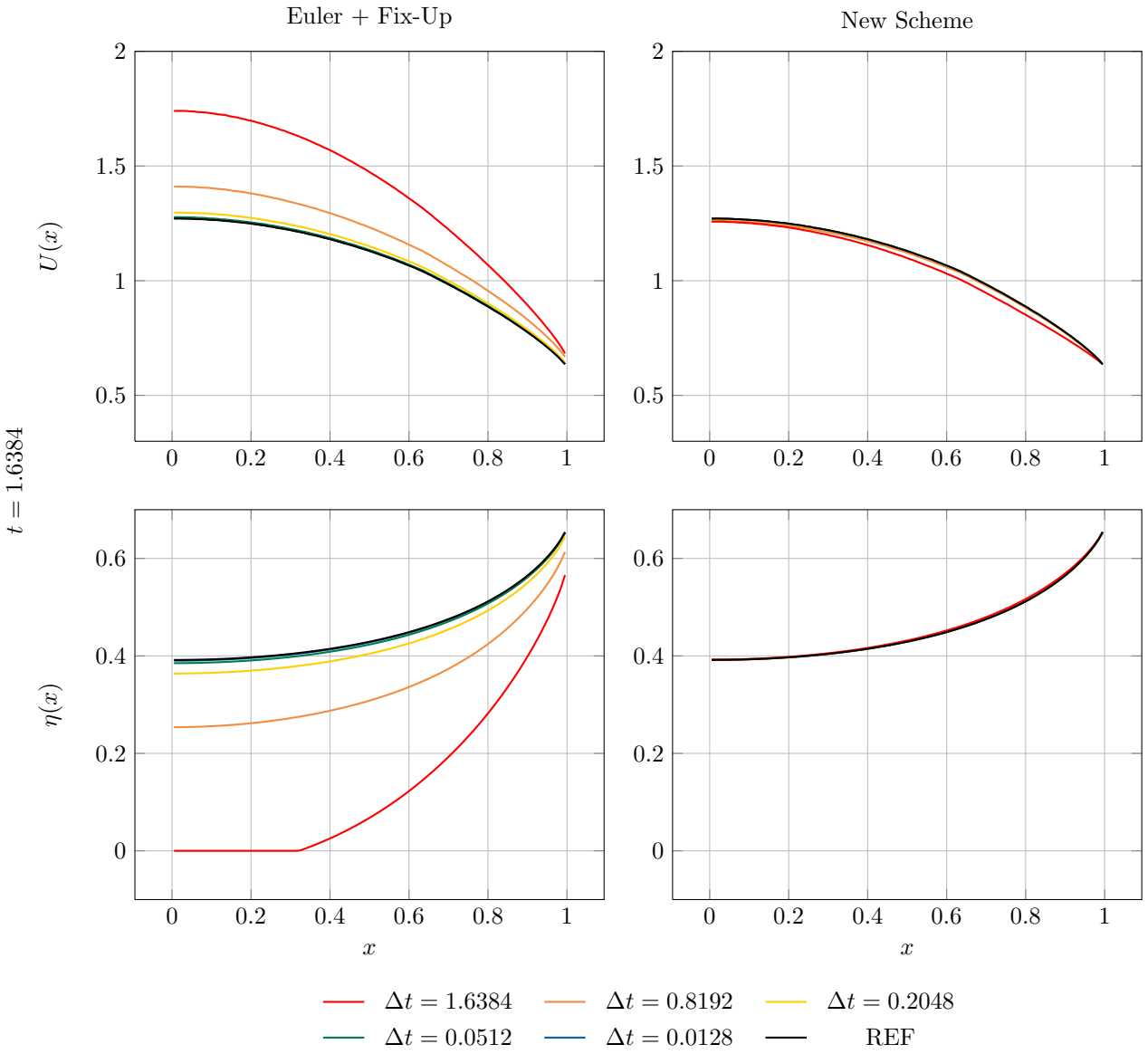

Fig. 12. Spatial profiles for the particle density $U(x, t = 1.6384) = \int u(x, t = 1.6384, \omega)\,\mathrm{d}\omega$ and component density $\eta(x, t = 1.6384)$ at $t = 1.6384$ for the classical scheme (left) and the new MC scheme (right) for $N_{MC} = 1677721600$ for the configuration of figure table 3.4 on page 12 with 100 cells.

equation is identical to the one performed in the previous section. The non-scalar equivalent of (3) is given by

$$\begin{cases} \partial_t U(t) = v \sum_{m=1}^{N} (\sigma_s^m - \sigma_t^m)\eta_m(t)U(t), \\ \partial_t \eta(t) = v\Sigma_R(\eta(t))U(t), \end{cases} \tag{11}$$

with $\eta = (\eta_1, ..., \eta_N)^t$, using once again the fact that $\forall m \in \{1, ..., N\}$, $\int P_s^m(\omega, \omega')\,\mathrm{d}\omega$, as in 4.

In order to apply the UMC methodology in the non-scalar case, we need to perform a change of variables in (11), more precisely we first need to rewrite the Bateman counterpart. To do so, let us first diagonalize the reaction matrix: $P\Lambda_R P^{-1} = \Sigma_R$ with $\Lambda_R = diag(\lambda_1, ..., \lambda_N)$ so that we have $\nu = P^{-1}\eta$ and $\eta = P\nu \implies \eta_m = \sum_{j=1}^{N} \alpha_{j,m}\nu_j$. Then performing a change of variables in (11) one gets

$$\begin{cases} \partial_t U(t) = v \sum_{m=1}^{N} (\sigma_s^m - \sigma_t^m) \left(\sum_{j=1}^{N} \alpha_{j,m}\nu_j(t) \right) U(t), \\ \partial_t \nu(t) = v\Lambda_R \nu(t)U(t). \end{cases} \tag{12}$$

It is now possible to express analytically each $\nu_j, j \in \{1, ..., N\}$

$$\nu_j(t) = \nu_j^0 e^{v\lambda_j \int_0^t U(s)\,\mathrm{d}s}, \forall j \in \{1, ..., N\}, \tag{13}$$

with $\nu^0 = P^{-1}\eta^0$. Let us now inject the $\nu_j(t), j \in \{1, ..., N\}$ in the first equation of (12):

$$\partial_t U(t) = -v \sum_{m=1}^{N} \sigma_a^m \left(\sum_{j=1}^{N} \alpha_{j,m} \nu_j^0 e^{v\lambda_j \int_0^t U(s)\,\mathrm{d}s} \right) U(t). \tag{14}$$

Equation (14) seems hard to solve with the occurence of three degrees of derivation $\partial_t U, U, \int U$. In order to obtain a more classical ODE, we rewrite

$$\partial_t U(t) = -v \sum_{m=1}^{N} \sigma_a^m \left(\sum_{j=1}^{N} \frac{\alpha_{j,m}}{v\lambda_j} \nu_j^0 \left(v\lambda_j U(t)\right) e^{v\lambda_j \int_0^t U(s)\,\mathrm{d}s} \right).$$

so that

$$\partial_t U(t) + v \sum_{m=1}^{N} \sigma_a^m \left(\sum_{j=1}^{N} \frac{\alpha_{j,m}}{v\lambda_j} \nu_j^0 \partial_t \left[e^{v\lambda_j \int_0^t U(s)\,\mathrm{d}s} \right] \right) = 0.$$

Integrating the previous equation between 0 and t leads to

$$U(t) + v \sum_{m=1}^{N} \sigma_a^m \left(\sum_{j=1}^{N} \frac{\alpha_{j,m}}{v\lambda_j} \nu_j^0 \left[e^{v\lambda_j \int_0^t U(s)\,\mathrm{d}s} \right] \right) = K_0 \text{ with } K_0 = U_0 + v \sum_{m=1}^{N} \sigma_a^m \sum_{j=1}^{N} \frac{\alpha_{j,m}}{v\lambda_j} \nu_j^0.$$

Let us introduce $\partial_t V(t) = U(t)$, we get a classical structure of an ODE

$$\partial_t V(t) + v \sum_{j=1}^{N} e^{v\lambda_j V(t)} \underbrace{\sum_{m=1}^{N} \sigma_a^m \frac{\alpha_{j,m}}{v\lambda_j} \nu_j^0}_{\beta_j} = K_0 \text{ or again } \partial_t V(t) - v \sum_{j=1}^{N} e^{v\lambda_j V(t)} \beta_j = K_0. \tag{15}$$

Equation (15) is the non-scalar counterpart of (3) which has been solved analytically in the previous sections. However without further assumptions, to our knowledge, no analytical solution of (15) is available and we were not able to build one as we did in section 2.1 on page 3.

Consequently, we will propose in next section a solver for (15) and explain how the approached V is used within a time dependent MC scheme. We will also discuss why we think the resulting unsplit MC scheme may remain relevant in term of computational efficiency.

4.2. *Details of the MC solver in the case of non-scalar Bateman system*

The aim of this section is to describe the key steps of the UMC solver in the case of non-scalar Bateman system. In particular, we propose a simple, time-step controlled, explicit Euler resolution for the ODE (15) of unknown V and detail how we merge it into the MC resolution.

4.2.1. *Numerical resolution of ODE (15) of unknown $V(t)$*

In order to apply the UMC solver with non-scalar Bateman systems, we expect the resolution of (15) to be stable and accurate. We suggest applying an explicit Euler scheme to (15) with a time step controlled by

$$t^{n+1} = t^n + \Delta t^n \quad \text{with} \quad \Delta t^n = \varepsilon_{acc} \frac{|V(t^n)|}{|V'(t^n)|} \quad \text{and} \quad \varepsilon_{acc} \leq 1 \tag{16}$$

Such choice allows a stable resolution of (15) and a controlled accuracy on the solution $\approx \mathcal{O}(\varepsilon_{acc})$. In the following, we introduce $V^n \approx V(t^n)$ the approximation of V at time t^n.

Equation (15) could have been solved in many other ways, some certainly being more efficient than the one presented here. Our choice is based on simplicity and efficient control of the accuracy. It also prevents from adding complexity in this paper.

4.2.2. *Time dependent characteristics and MC resolution*

The approximation V^n allows on the fly estimation of matter evolution inside the MC solver itself. To clarify this process, we will first remind the main features of the MC resolution of the transport equation with time dependent characteristics [3] .

As emphasized in section section 3.1 on page 8, the transport equation with time dependent characteristics can be written as an expectation:

$$u(x,t,\omega) = \mathbb{E}\left[u_0(x - v\omega t, \omega)e^{-\int_0^t v\sigma_a(\alpha)\,\mathrm{d}\alpha}\mathbf{1}_{[t,\infty[}(\mathcal{S}) + u(x - v\omega\mathcal{S}, t-\mathcal{S}, W')e^{-\int_{t-\mathcal{S}}^t v\sigma_a(\alpha)\,\mathrm{d}\alpha}\mathbf{1}_{[0,t]}(\mathcal{S})\right] \tag{17}$$

where $W' \sim P_s(t-\mathcal{S},\omega,W')$ and $\mathcal{S} \sim \mathcal{E}_t(v\sigma_s)$ with $\mathcal{E}_t(v\sigma_s)$ denoting the probability law of the random variable having for pdf

$$f(s) = \mathbf{1}_{[0,\infty]}(s)v\sigma_s(t-s)e^{-\int_0^s v\sigma_s(t-\beta)\,\mathrm{d}\beta}.$$

Note that on one hand these probability laws imply no assumption on the expression of $(\sigma_\alpha)_{\alpha\in\{a,s,t\}}$. One the other hand, as $V(t)$ is approximated, we will have to incorporate the resolution of (15) into the computation process of interaction time $\mathcal{S}$ and MC particles weight evolution with time.

– **Sampling the interaction time $\mathcal{S}$ from the pdf f**: As in section 3.2 on page 9, we begin applying the cdf inversion method :

$$\mathcal{U} = F(\mathcal{S}) = \int_{-\infty}^{\mathcal{S}} f(s)\,\mathrm{d}s = 1 - e^{-\int_0^{\mathcal{S}} v\sigma_s(t-\beta)\,\mathrm{d}\beta},$$

leading to

$$-\ln(\mathcal{U}) = \int_0^{\mathcal{S}} v\sigma_s(t-\beta)\,\mathrm{d}\beta = -\ln(\mathcal{U}) = \int_{t-\mathcal{S}}^t v\sigma_s(\alpha)\,\mathrm{d}\alpha.$$

This formula is very general in the sense that it does not take into account a particular dependence of σ_s with respect to time. We now use the structure of the Bateman system for the expression of $\sigma_s(t)$:

$$-\ln(\mathcal{U}) = \int_{t-\mathcal{S}}^t v\sum_{m=1}^M \sigma_s^m\eta_m(\alpha)\,\mathrm{d}\alpha = \int_{t-\mathcal{S}}^t v\sum_{m=1}^M\sum_{j=1}^M \sigma_s^m\alpha_{j,m}\nu_j^0 e^{v\lambda_j V(\alpha)}\,\mathrm{d}\alpha = \int_{t-\mathcal{S}}^t I_s(V(\alpha))\,\mathrm{d}\alpha.$$

This last expression could be discouraging as it implies estimating the integral of a rather complex function of V. However, as we chose an explicit Euler solver in order to estimate the evolution of V, we may benefit from the intermediate values computed for the sake of precision and stability. Here are the key steps we suggest to estimate the sampling of $\mathcal{S}$:

(i) First, sample from a uniform law $\mathcal{U}$ on $[0,1]$ and compute $-\ln(\mathcal{U})$.

(ii) Apply one iteration of an explicit Euler scheme with adaptive time step as described in section 4.2.1 on the previous page. Remind that $V(0) = 0$ and that $\partial_t V(t) = U(t) > 0$ so that $V(t)$ is monotone, increasing and positive. This leads to a first approximation V^1 at $t^1 = 0 + \Delta t^1$.

(iii) apply a trapezoidal rule in order to approximate $\int_0^{t^1} I_s(V(\alpha))\,\mathrm{d}\alpha \approx \frac{1}{2}(I_s(V^0) + I_s(V^1))\Delta t^1 = I_s^1$

(iv) repeat the two previous steps and build the approximation V^n at iteration n together with the approximation of the integral

$$I_s^n = \sum_{i=1}^n \frac{1}{2}(I_s(V^{i-1}) + I_s(V^i))\Delta t^i \quad \text{until} \quad -\ln(\mathcal{U}) < I_s^n.$$

(v) t^n is then an approximation of $\mathcal{S} = t^n + \mathcal{O}(\varepsilon_{acc})$ of order to accuracy $\mathcal{O}(\varepsilon_{acc})$.

We now suppose we have an approximation of relative accuracy $\mathcal{O}(\varepsilon_{acc})$ for the sampling of the interaction time $\mathcal{S}$. Let us now detail how we compute the weight modification for each MC particles.

– **Weight modification of the MC particles**: The evolution of a MC particle weight is ruled by the factor:

$$K(t, t-\mathcal{S}) = e^{-v\int_{t-\mathcal{S}}^t \sigma_a(\alpha)\,\mathrm{d}\alpha}.$$

[3] We refer to [19] for more details

Once again, this formula is general and considering evolving matter densities η_m, we get

$$K(t, t-\mathcal{S}) = e^{-v\int_{t-\mathcal{S}}^{t} \sum_{m=1}^{M} \sigma_a^m \eta_m(\alpha)\,\mathrm{d}\alpha}$$

or expressing η thanks to ν (see (12))

$$K(t, t-\mathcal{S}) = e^{\int_{t-\mathcal{S}}^{t} -v \sum_{m=1}^{M}\sum_{j=1}^{M} \sigma_a^m \alpha_{j,m}\nu_j^0 e^{v\lambda_j V(\alpha)}\,\mathrm{d}\alpha} = e^{-\int_{t-\mathcal{S}}^{t} I_a(V(\alpha))\,\mathrm{d}\alpha},$$

We would like to emphasize that the above expression can be considerably simplified: we get from (15) that

$$\frac{\mathrm{d}V}{-v\sum_{j=1}^{M}\sum_{m=1}^{M} \sigma_a^m \frac{\alpha_{j,m}}{v\lambda_j}\nu_j^0 e^{v\lambda_j V} + K_0} = \mathrm{d}\alpha,$$

and using the previous variable change in the exponential term in the weight modification we have:

$$-\int_{t-\mathcal{S}}^{t} I_a(V(\alpha))\,\mathrm{d}\alpha = \int_{V(t-\mathcal{S})}^{V(t)} \frac{\left[-v\sum_{m=1}^{M}\sum_{j=1}^{M} \sigma_a^m \alpha_{j,m}\nu_j^0 e^{v\lambda_j V}\right]}{-v\sum_{j=1}^{M}\sum_{m=1}^{M} \sigma_a^m \frac{\alpha_{j,m}}{v\lambda_j}\nu_j^0 e^{v\lambda_j V} + K_0}\,\mathrm{d}V.$$

If we now introduce

$$L_a(V) = -v\sum_{j=1}^{M}\sum_{m=1}^{M} \sigma_a^m \frac{\alpha_{j,m}}{v\lambda_j}\nu_j^0 e^{v\lambda_j V} + K_0 \text{ with } L_a'(V) = -v\sum_{j=1}^{M}\sum_{m=1}^{M} \sigma_a^m \alpha_{j,m}\nu_j^0 e^{v\lambda_j V},$$

we obtain

$$-\int_{t-\mathcal{S}}^{t} I_a(V(\alpha))\,\mathrm{d}\alpha = \int_{V(t-\mathcal{S})}^{V(t)} \frac{L_a'(V)}{L_a(V)}\,\mathrm{d}V = \ln\left(\frac{L_a(V(t))}{L_a(V(t-\mathcal{S}))}\right),$$

or again

$$K(t, t-\mathcal{S}) = e^{-\int_{t-\mathcal{S}}^{t} I_a(V(\alpha))\,\mathrm{d}\alpha} = \frac{L_a(V(t))}{L_a(V(t-\mathcal{S}))} = \frac{U(t)}{U(t-\mathcal{S})}, \tag{18}$$

The above expression ensures that only two evaluations $V(t), V(t-\mathcal{S})$ are enough in order to compute the weight modification once $\mathcal{S}$ is approximated. Note that the particle weight modification has in fact the same structure in the degenerate case (10) as in the non-degenerate (18).

– **Sampling of the** $W' \sim P_s(t-\mathcal{S}, \omega, W')$: The sampling of $W' \sim P_s(t-\mathcal{S}, \omega, W')$ is in fact classical enough. Indeed, the definition of P_s gives

$$P_s(t-\mathcal{S}, \omega, \omega') = \frac{\sigma_s(t-\mathcal{S}, \omega, \omega')}{\sigma_s(t-\mathcal{S})} = \frac{\sum_{m=1}^{M} \sigma_s^m(\omega, \omega')\eta^m(t-\mathcal{S})}{\sum_{m=1}^{M} \sigma_s^m \eta^m(t-\mathcal{S})}, \tag{19}$$

with $\eta^m(t-\mathcal{S}), \forall m \in \{1, ..., M\}$ being closely related to $V(t-\mathcal{S})$ which has been previously estimated as $\forall m \in \{1, ..., M\}$ we have

$$\eta^m(t-\mathcal{S}) = \sum_{j=1}^{M} \alpha_{j,m}\nu_j^0 e^{v\lambda_j V(t-\mathcal{S})}.$$

The sampling of W' is then easy since the η^m have already been estimated for interaction time.

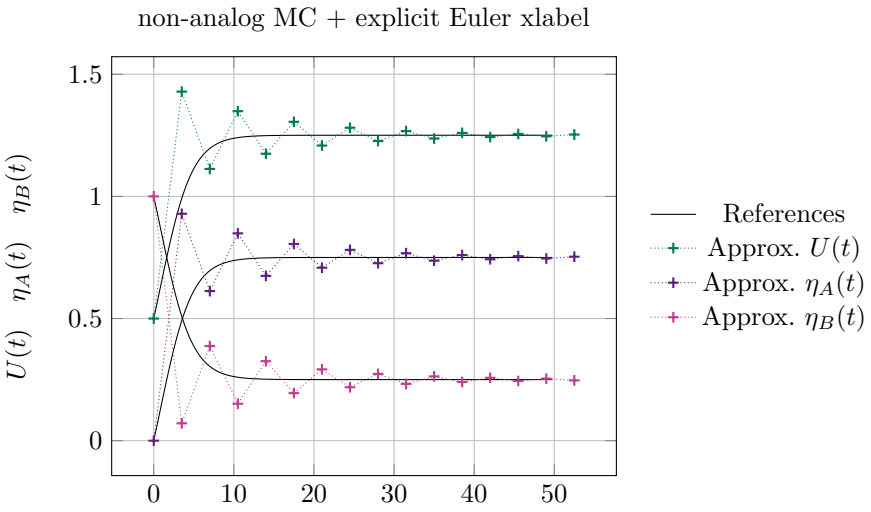

Fig. 14. Time evolutions of the computed $U(t), \eta_A(t), \eta_B(t)$ with the classical solver (non-analog MC + explicit Euler) for the resolution of the problem of section 4.3 for two time discretizations $\Delta t = 4.54$ and $\Delta t = 0.5$ and $N_{MC} = 1$.

– **Crossing cell boundaries** Once again, rigorously speaking, we should here describe how we proceed when a MC particle crosses the boundary between two cells. Please report to section B on page 34 for the general study.

Once the above elements are described, we consider the UMC solver has been characterized in application to the monokinetic transport equation coupled with the non-scalar Bateman system. In the next section, we apply this solver to a new test-problem.

4.3. *Numerical test-problem 1g2r-h in the case of non-scalar Bateman system*

In this section, we apply the UMC solver to a new test-problem with 1 group (1g) and a 2 materials vector $\eta = (\eta_A, \eta_B)^t$ (2r) and a 2×2 reaction matrix in a homogeneous configuration (h) for which we can introduce

$$\Sigma_R = \begin{pmatrix} -\sigma_R^0 & +\sigma_R^1 \\ +\sigma_R^0 & -\sigma_R^1 \end{pmatrix} = P \Lambda_R P^{-1} = P \begin{pmatrix} 0 & 0 \\ 0 & -\sigma_R^0 - \sigma_R^1 \end{pmatrix} P^{-1}. \tag{20}$$

where Λ_R is the diagonal matrix of Σ_R: we here insist on the fact that the algorithm only needs the diagonalization of the reaction matrix at the beginning of the computation once and for all.

U_0	η_A^0	η_B^0	v	$\sigma_t^{A,B}$	$\sigma_s^A \vert \sigma_s^B$	$\sigma_R^0 \vert \sigma_R^1$	left BC	right BC
0.50	0.00	1.00	1.00	1.00	0.90|1.30	0.10|0.30	specular	1g2r-h : specular 1g2r-nh : free

Fig. 13. Parameters for the test 1g2r-h.

Concerning the numerical values used in this section we consider table 13. According to it the material A is absorbing as $\sigma_s^A < \sigma_t^A$ whereas B is multiplicative. Initially, there is a certain density U_0 of particles and A is absent from the composition of the medium. In the following, we solve the above problem with both the classical scheme and the UMC one we presented in the previous section.

4.4. *Numerical resolution of problem 1g2r-h with the* **classical** *solver*

In this section, we first solve the above problem with the reference configuration : the non-analog scheme of appendix A.3 (transport phase) together with the explicit Euler scheme of section 2.3 on page 4 (Bateman phase). The time evolutions of the computed $U(t), \eta_A(t), \eta_B(t)$ are displayed in fig. 14 for two time discretizations $\Delta t = 4.54$ and $\Delta t = 0.5$ and $N_{MC} = 1$ with time going from $t = 0$ to $t = 50$.

First, in fig. 14, we observe that for a fine time discretization $\Delta t = 0.5$, the solutions are smooth with respect to time and that a steady state is set after $t \approx 15$. However, for $\Delta t = 4.54$, the solutions exhibit an oscillatory behaviour. Larger time steps would have lead to even worse oscillations/instabilities.

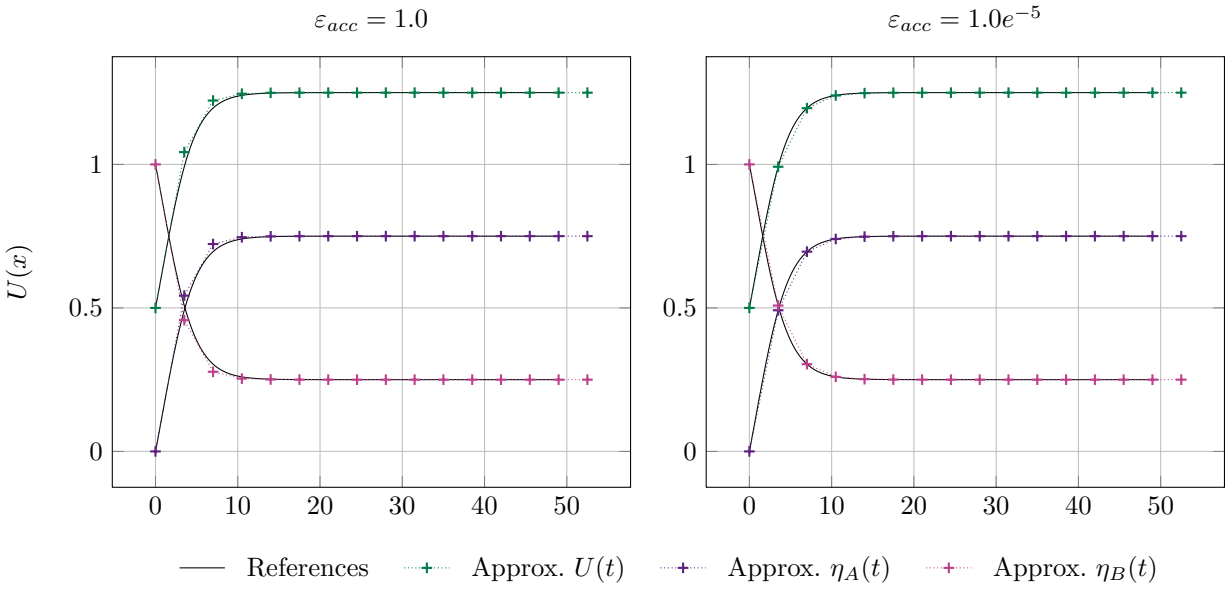

Fig. 15. The two pictures present the resolutions with the new MC solver for two different levels of accuracy for the resolution of (15): first $\varepsilon_{acc} = 1.0$ and then $\varepsilon_{acc} = 1.0e^{-5}$.

4.5. *Numerical resolution of problem 1g2r-h with the UMC solver*

On the same problem, keeping exactly the same discretization parameters, the application of the new scheme characterized in section 4.2 on page 16 requires an additional parameter. In fact, we remind that the adaptive time-step control is governed by ε_{acc}. In fig. 14 on the previous page we present the results obtained with UMC with $\Delta t = 4.54$, compared to the same reference as above, to analyze the impact of ε_{acc}.

As ε_{acc} sets the accuracy of the time resolution of ODE (15) of unknown $V(t)$ (detailed in section 4.2.1 on page 16), results are better with $\varepsilon_{acc} = 1.0e^{-5}$ than with $\varepsilon_{acc} = 1$. However, none of these leads to instability, and the steady-state is well captured. The numerical strategy allows ensuring a control of the accuracy of the resolution of (15) leading to stability for the full problem together with an accurate resolution.

Note that in this section, we relied on the diagonalization of the reaction matrices and do not intend to deal with a badly conditioned one (ratio of the highest eigenvalue on the lowest one greater than machine accuracy). In the general case, as detailed in section 5 on the next page, we will avoid this diagonalization step.

4.6. *Numerical resolution of problem 1g2r-nh (non-homogeneous) with both solvers*

In the same manner as in the previous section 3.4 on page 12, the next step consists in changing slightly the test problem by imposing a vacuum boundary condition on the right hand side of the simulation domain. Doing so, we now consider test-problem 1g2r-nh instead of 1g2r-h cf table 13 on the previous page, and compare the time evolutions and spatial profiles of the different quantities.

In fig. 16 on the next page we present the time evolutions of the particle and material densities on test problem 1g2r-nh for several time discretization values. These are obtained with the classical scheme and the UMC scheme of section 4.2 on page 16. Concerning the UMC scheme, only the coarser discretization $\Delta t = 6 = T_{final}$ gives unsatisfactory results whereas the classical scheme needs $\Delta t = 0.0625$ to obtain equivalent accuracy. Note that for this problem 1g2r-nh, we used $\varepsilon_{acc} = 1.e^{-5}$.

Fig. 17 on page 22 presents the spatial profiles of material densities for several time discretization values with both schemes. Once again, the convergence is way faster with the UMC scheme as all chosen time-steps except the coarser one ($\Delta t = 3$) allow recovering with a good agreement the reference profile obtained with the finest discretization of the classical scheme. Concerning the coarser time-step ($\Delta t = 3$), we insist on the fact that such discrepancy was not observable on the homogeneous problem in the same conditions: spatial effects in the transport phase may still impose limitations on the time step for the sake of accuracy.

In this section, we extended the new MC scheme to monokinetic transport coupled to Bateman systems (multi-materials): it turned out that we relied on a solver (explicit Euler one) in order to approximate up to accuracy ε_{acc} the MC scheme quantities (such as interaction sampling, and particle weight evolution). However, the method once again

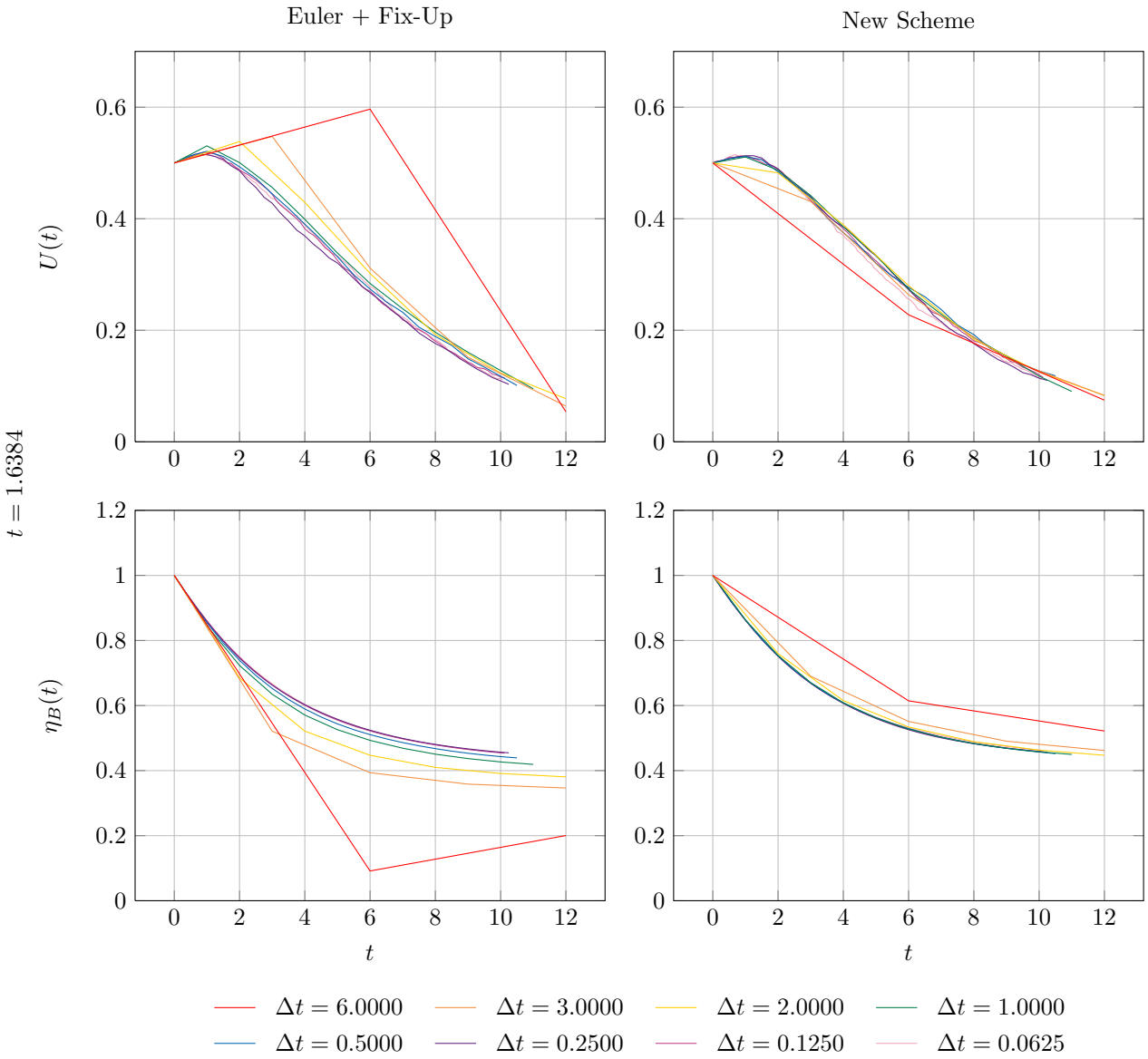

Fig. 16. Time evolution of $U(t)$ and $\eta_B(t)$ for the configuration of section 4.3 on page 19 for the classical scheme (left) and the new MC scheme (right) for several time discretizations Δt and $N_{MC} = 5000$. A common scale is used for both schemes.

does not exhibit numerical instabilities (i) and is less sensitive to time discretization (ii).

5. Transport with energy dependence coupled to the Bateman system

Let us now tackle the extension of our new scheme to the case of energy dependence. According to the type of particle considered, the problem can be written with a dependence to velocity, frequency or directly energy. As we referred mainly to burn-up issues where neutrons are considered, we are going to treat with a velocity dependence. The difficulty of this extension mainly consists in the fact that in the general case (velocity dependence + non scalar Bateman equation) the reaction matrix do not commute/are not diagonalizable in the same basis, i.e. in general $\Sigma_R(v)\Sigma_R(v') \neq \Sigma_R(v')\Sigma_R(v)$. This leads to a less elegant resolution scheme than in the last sections (where we were able to solve a scalar ODE with respect to the variable $V(t)$) but still an efficient and very general one which we will detail here.

5.1. *Multi-group discretization*

There are two main ways to solve the above system (1), the multi-group approach [16, 25, 3] and the punctual one (a.k.a. continuous energy). A multi-group discretization of the velocity dimension first consists in the choice of a weighting

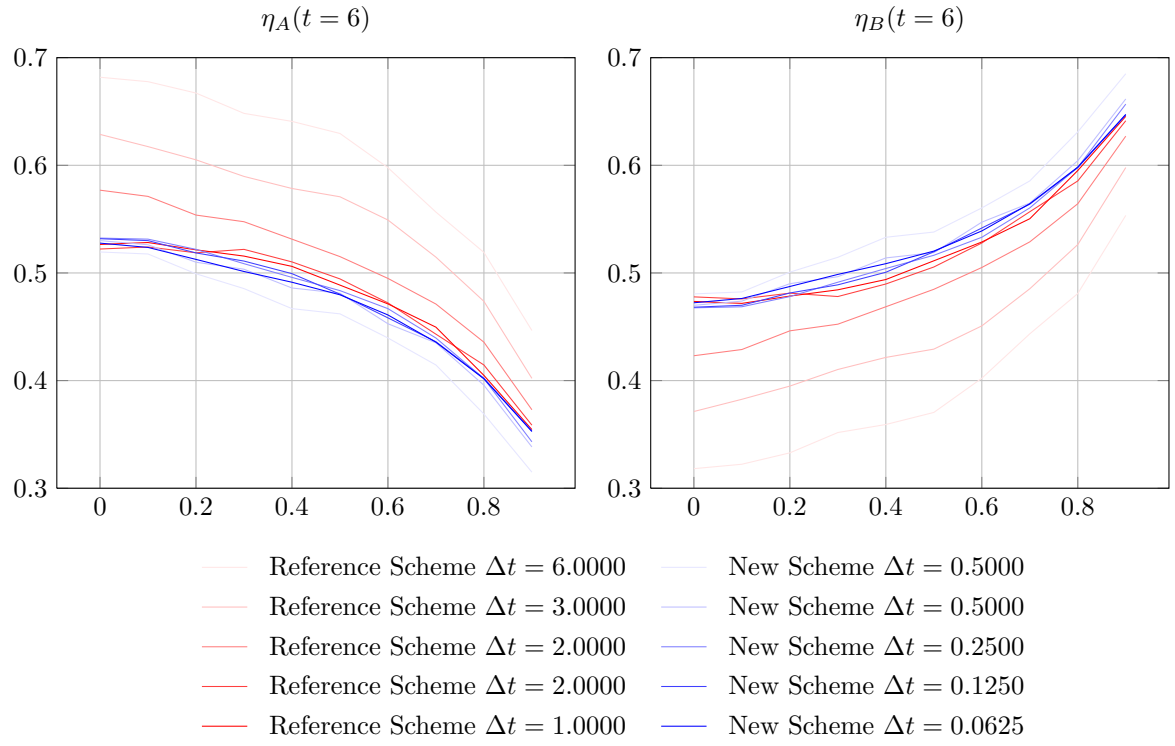

Fig. 17. Comparison of the spatial profiles for the component densities $\eta_A(x,t=6), \eta_B(x,t=6)$ at $t=6$ for the classical scheme scheme and the new MC scheme for $N_{MC}=5000$ for the configuration of section 4.3 on page 19 for 4 time-steps $\Delta t = 2.000$, $\Delta t = 1.000$, $\Delta t = 0.125$ and $\Delta t = 0.0625$ with 10 cells.

flux $(\phi_g(v))_{g\in\{1,...,G\}}$, $\phi_g(v)$ being an approximation of the solution between the boundaries of the group g. Then it consists in preparing the data $(\sigma_\alpha(v))_{\alpha\in\{s,t,R\}}$ with respect to velocity dependence and solve the system in the vector of unknowns $(u^1,...,u^G)^t$ where $u^g(x,t,\omega)=\int u(x,t,v,\omega)\phi_g(v)\,\mathrm{d}v$ so that $\int u(x,t,v,\omega)\,\mathrm{d}v \approx \sum_{g=0}^{G} u_g(x,t,\omega)$. Multi-group characteristics consequently need a preprocessing of the data. A punctual approach is simpler in its description as it uses raw data $(\sigma_\alpha(v))_{\alpha\in\{s,t,R\}}$ at point v (or an interpolation between available punctual values). In general, deterministic solvers need multi-group preprocessing whereas MC methods can easily handle both. Of course, the multi-group approach converges toward the punctual one as the number of groups increases. In this paper, we focus on the multi-group approach because it can be applied to both deterministic and MC solvers.

The multi-group counterpart of (1) is given by [4]

$$\begin{cases} \forall g \in \{1,...,G\}, \\ \partial_t u_g(x,t,\omega) + v_g\omega\nabla u_g(x,t,\omega) + v_g\sigma_t^g(\eta(x,t))u_g(x,t,\omega) = v_g\displaystyle\sum_{g'=0}^{G}\int \sigma_s^{g',g}(\eta(x,t),\omega',\omega)u_{g'}(x,t,\omega')\,\mathrm{d}\omega', \\ \partial_t\eta(x,t) = \displaystyle\sum_{g=0}^{G} v_g\Sigma_g^R(\eta(x,t))\int u_g(x,t,\omega')\,\mathrm{d}\omega', \end{cases} \tag{21}$$

and can be rewritten in a vectorial form as

$$\begin{cases} \partial_t U(x,t,\omega) + V\omega\nabla U(x,t,\omega) + V\Sigma_t(\eta(x,t))U(x,t,\omega) = V\displaystyle\int \Sigma_s(\eta(x,t),\omega',\omega)U(x,t,\omega')\,\mathrm{d}\omega', \\ \partial_t\eta(x,t) = V\Sigma^R(\eta(x,t))\displaystyle\int U(x,t,\omega')\,\mathrm{d}\omega'. \end{cases} \tag{22}$$

where $U(x,t,\omega)=(u^1(x,t,\omega),...,u^G(x,t,\omega))^t$, $V = diag_{g\in\{1,...,G\}}(v_g)$ and $\Sigma_t = diag_{g\in\{1,...,G\}}(\sigma_t^g)$ where the notation $diag_{l\in\{1,...,L\}}(a_l)$ stands for the diagonal matrix with eigenvalues $(a_l)_{l\in\{1,...,L\}}$. Σ_s is considered as a full matrix of general term $\sigma_s^{g',g}(x,t,\omega',\omega)$. Besides, we remind that the dependencies with respect to x,t of the $(\Sigma_\alpha)_{\alpha\in\{t,s,R\}}$ are isolated in the vector of materials densities $\eta(x,t)$, i.e. we have the following notations $\Sigma_\alpha(x,t)=\Sigma_\alpha(\eta(x,t))=\sum_{m=1}^{M}\Sigma_\alpha^m\eta_m(x,t)$ where Σ_α^m correspond to the $G\times G$ matrix for material m.

[4] Note that we do not insist on the construction of system (21), it is established in many references, see for example [16, 25, 3].

5.2. *Methodology for introducing the Unsplit MC scheme*

5.2.1. *First key step of the Unsplit MC scheme: a change of variable*

Until this point we used to present the UMC scheme as a MC method with time dependent characteristics themselves governed by the resolution of a local problem. Indeed, we will now show that it corresponds more generally to a change of variable. Let us introduce the vectors z, q of sizes G and M solutions of the ODE:

$$\begin{cases} \partial_t z(x,t) = -V\Sigma_a(q(x,t))z(x,t) & \text{with} \quad z(x,0) = \displaystyle\int U(x,0,\omega')\,\mathrm{d}\omega', \\ \partial_t q(x,t) = V\Sigma_R(q(x,t))z(x,t) & \text{with} \quad q(x,0) = \eta(x,0), \end{cases} \tag{23}$$

in which x is a parameter, where $\Sigma_s = \int \Sigma_s(\omega',\omega)\,\mathrm{d}\omega'$ and $\Sigma_a = \Sigma_t - \Sigma_s$. Let us now introduce the diagonal matrix $Z = I \times z = diag_{g\in\{1,\dots,G\}}(z_g)$. We perform a change of variable in (22) by introducing the vector f such that $U(x,t,\omega) = Z(x,t)f(x,t,\omega)$. Injecting the change of variable in (22) and using the fact that Z is invertible leads to

$$\begin{cases} \partial_t f(x,t,\omega) + V\omega\nabla f(x,t,\omega) + \\ \left[Z^{-1}(x,t)V\Sigma_t(\eta(x,t))Z(x,t) + Z^{-1}(x,t)\partial_t Z(x,t) + Z^{-1}(x,t)V\omega\nabla Z(x,t)\right] f(x,t,\omega) \\ = \displaystyle\int Z^{-1}(x,t)V\Sigma_s(\eta(x,t),\omega',\omega)Z(x,t)f(x,t,\omega')\,\mathrm{d}\omega', \\ \partial_t\eta(x,t) = V\Sigma^R(\eta(x,t)) \displaystyle\int U(x,t,\omega')\,\mathrm{d}\omega'. \end{cases} \tag{24}$$

As we noted before, $Z, Z^{-1}, V, \Sigma_s, \Sigma_a, \Sigma_t$ do not necessarily commute making calculations more complex than in 3 or 4. The first part of equation (23) allows writing the general term of the *diagonal* matrix $Z^{-1}\partial_t Z$

$$\left[Z^{-1}(x,t)\partial_t Z(x,t)\right]_{g,g} = -v_g \sum_{g'=1}^{G} \sigma_a^{g,g'}(q(x,t))\frac{z_{g'}(x,t)}{z_g(x,t)} = -v_g\sigma_t^g + v_g \sum_{g'=1}^{G} \sigma_s^{g,g'}(q(x,t))\frac{z_{g'}(x,t)}{z_g(x,t)}.$$

Let us introduce few notations: first the *diagonal* matrix $\Lambda_s(Z(x,t),q(x,t))$ of general term

$$\lambda_s^g(Z(x,t),q(x,t)) = \sum_{g'=1}^{G} \sigma_s^{g,g'}(q(x,t))\frac{z_{g'}(x,t)}{z_g(x,t)}.$$

Secondly, we define $M_s(Z(x,t),\eta(x,t),\omega',\omega) = Z^{-1}(x,t)\Sigma_s(\eta(x,t),\omega',\omega)Z(x,t)$. From this point, it is convenient noticing that $M_s(Z(x,t),\eta(x,t),\omega,\omega')$ can be written $M_s(Z(x,t),\eta(x,t),\omega',\omega) = \Lambda_s(Z(x,t),\eta(x,t))P_s(Z(x,t),\eta(x,t),\omega',\omega)$ [5] using the formentionned relations between Σ_s and $\Sigma_s(\omega',\omega)$. Now, plugging the above expressions in (24) we obtain

$$\begin{cases} \partial_t f(x,t,\omega) + V\omega\nabla f(x,t,\omega) + \begin{pmatrix} V\Sigma_t\left(\eta(x,t) - q(x,t)\right) \\ +Z^{-1}(x,t)V\omega\nabla Z(x,t) \\ +V\Lambda_s(Z(x,t),q(x,t)) \end{pmatrix} f(x,t,\omega) \\ = V\Lambda_s(Z(x,t),\eta(x,t)) \displaystyle\int P_s(Z(x,t),\eta(x,t),\omega',\omega)f(x,t,\omega')\,\mathrm{d}\omega', \\ \partial_t\eta(x,t) = V\Sigma^R(\eta(x,t)) \displaystyle\int U(x,t,\omega')\,\mathrm{d}\omega'. \end{cases} \tag{25}$$

The factor of $f(x,t,\omega)$ is a sum of 3 terms and we will spend some time detailing their discretization in the following. Note also that the change of variable (23) is closely related to Quasi-Static methods [11, 12, 4, 18] with dependencies with respect time, space and velocity (or energy). We put forward the fact that until this point, the change of variable is exact. Let us now introduce some discretization hypothesis necessary to describe our new MC scheme applied to the multi-group problem (25).

5.2.2. *Space and time discretization hypothesis*

The simulation domain $\mathcal{D}$ approximated by N_x cells (whatever the geometry, 1D, 2D, 3D...) such that

$$\mathcal{D} = \bigcup_{i\in\{1,\dots,N_x\}} \mathcal{D}_i.$$

[5] where basically $P_s(Z(x,t),\eta(x,t),\omega',\omega)$ is defined by $P_s(Z(x,t),\eta(x,t),\omega',\omega) = \Lambda_s^{-1}(Z(x,t),\eta(x,t))M_s(Z(x,t),\eta(x,t),\omega',\omega)$.

We also suppose $t \in [0, \Delta t]$ with $\Delta t > 0$. The first assumption concerns the vector $(z(x,t), q(x,t))$. Indeed, we suppose it is constant with respect to x in each cell $(\mathcal{D}_i)_{i\in\{1,...,N_x\}}$. In other words, we have

Hypothesis 1 $\forall x \in \mathcal{D}, \forall t \in [0, \Delta t], \forall i \in \{1, ..., N_x\}$

$$\begin{cases} z(x,t) = z_i(t)\mathbf{1}_{\mathcal{D}_i}(x), \\ q(x,t) = q_i(t)\mathbf{1}_{\mathcal{D}_i}(x). \end{cases}$$

This implies that $z_i(t) = \frac{1}{|\mathcal{D}_i|}\int_{\mathcal{D}_i} z(x,t)\,\mathrm{d}x$ and $q_i(t) = \frac{1}{|\mathcal{D}_i|}\int_{\mathcal{D}_i} q(x,t)\,\mathrm{d}x$. The change of variable (23) under hypothesis 1 now becomes (with $i \in \{1, ..., N_x\}$):

$$\begin{cases} \partial_t z_i(t) = -V\Sigma_a(q_i(t))z_i(t) \quad \text{with} \quad z_i(0) = \dfrac{1}{|\mathcal{D}_i|}\displaystyle\int_{\mathcal{D}_i}\int U(x,0,\omega')\,\mathrm{d}\omega'\,\mathrm{d}x, \\ \partial_t q_i(t) = V\Sigma_R(q_i(t))z_i(t) \quad \text{with} \quad q_i(0) = \dfrac{1}{|\mathcal{D}_i|}\displaystyle\int_{\mathcal{D}_i}\eta(0,x)\,\mathrm{d}x. \end{cases} \tag{26}$$

Consequently, we introduce $Z(x,t) = Z_i(t)\mathbf{1}_{\mathcal{D}_i}(x) = diag_{g\in\{1,...,G\}}(z_{i,g}(t))\mathbf{1}_{\mathcal{D}_i}(x)$. In practice in the following, in order to solve (26), we rely on the same explicit Euler scheme introduced in section 4.2.1 on page 16, the main difference being the ODE (26) is not scalar anymore, (cf (15)). The initial sampling of the MC particles ensures the spatial and angular distribution of the initial condition: the weight of each particle in the cell i in the group g at $t = 0$ is given by

$$w_{p\in\mathcal{D}_i, p\in g}(0) = \frac{1}{N_{MC}^{g,i}} \text{ where } N_{MC}^{i,g} = \frac{N_{MC}}{GN_x} \text{ denotes the number of MC particles belonging to } \mathcal{D}_i \text{ and to the group } g$$

so that $\sum_{p\in\mathcal{D}_i, p\in g} w_p(0)z_{g,i}(0) = z_{g,i}(0)$ and $\sum_{p\in\mathcal{D}_i, p\in g} w_p(0) = \dfrac{1}{|\mathcal{D}_i|}\displaystyle\int_{\mathcal{D}_i}\int f_g(x,0,\omega)\,\mathrm{d}\omega\,\mathrm{d}x = 1$, where we applied the abusive notations $p \in g$ for the MC particle of group g (idem for the other fields).

We now consider each of the three terms in factor of $f(x,t,\omega)$ in (25). To deal with these ones, we will have to make an additional assumption. In the following, we will intensively use the fact that we describe events occurring to MC particles. However, the resolution of the modified transport equation by a MC method will be mainly detailed in paragraph 5.2.5.

5.2.3. *The Unsplit MC scheme's main hypothesis*

Let us consider the first term $V\Sigma_t\left(\eta(x,t) - q(x,t)\right)$ in (25) and more precisely, the time evolution of term $\eta(x,t) - q(x,t)$: $\forall x \in \mathcal{D}, \forall t \in [0, \Delta t]$

$$\begin{aligned} \partial_t\left(\eta(x,t) - q(x,t)\right) &= v\Sigma^R\left(\eta(x,t)Z(x,t)\int f(x,t,\omega)\,\mathrm{d}\omega - q(x,t)Z(x,t)\mathcal{I}_G\right), \\ \partial_t\left(\eta(x,t) - q(x,t)\right) &= v\Sigma^R\left(\eta(x,t)\int f(x,t,\omega)\,\mathrm{d}\omega - q(x,t)\mathcal{I}_G\right)Z(x,t), \end{aligned} \tag{27}$$

where $\mathcal{I}_G = (\underbrace{1, ..., 1}_{G})^t$. During one time step, we typically will not have access to $\int f_g(x,t,\omega)\,\mathrm{d}\omega$, $\forall g \in \{1, ..., G\}, \forall x \in \mathcal{D}, \forall t \in [0, \Delta t]$, consequently, we will assume that (classical hypothesis in QS applications [11, 12, 4, 18])

Hypothesis 2

$$\forall g \in \{1, ..., G\}, \forall x \in \mathcal{D}, \forall t \in [0, \Delta t], \forall \omega \;\; f_g(x,t,\omega) \approx f_g(x,0,\omega) = 1.$$

This implies that $\forall x \in \mathcal{D}, \forall t \in [0, \Delta t]$ $\int f(x,t,\omega)\,\mathrm{d}\omega \approx \int f(x,0,\omega)\,\mathrm{d}\omega = \mathcal{I}_G$ and consequently (27) will simplify to

$$\partial_t\left(\eta(x,t) - q(x,t)\right) \approx v\Sigma^R Z(x,t)\left(\eta(x,t) - q(x,t)\right), \tag{28}$$

whose solution is given by

$$\eta(x,t) - q(x,t) \approx (\eta(x,0) - q(x,0))e^{\int_0^t v\Sigma^R Z(x,s)\,\mathrm{d}s}.$$

By construction of the change of variable (23) at the basis of the methodology, $\eta(x,0) - q(x,0) = 0$ which implies $\forall x \in \mathcal{D}, t \in [0, \Delta t]$, $\eta(x,t) - q(x,t) \approx 0$ and consequently $\forall x \in \mathcal{D}, t \in [0, \Delta t]$,

$$V\Sigma_t\left(\eta(x,t) - q(x,t)\right) \approx 0.$$

With regard to the latter hypothesis, let us only emphasize that:

- All $\approx$ of this section can be replaced by $=$ if the problem is homogeneous (indeed homogeneous$\Rightarrow \forall x \in \mathcal{D}, \forall t \in [0, \Delta t]$ $\int f(x,t,\omega)\,\mathrm{d}\omega = \mathcal{I}_G$): this is why in the cases of section 3 on page 8 and section 4 on page 14 where there was only one cell and the particles could not exit it, the new MC scheme allowed recovering exactly the analytical solutions.

– If the problem is not homogeneous, then spatial effects may have an important impact on accuracy. An illustration of such a situation was given in section 4.6 on page 20. Even if these considerations go beyond the aim of this paper, we mention that a control of time step would be necessary to preserve accuracy in such a situation. It may look like a CFL condition, however we prefer not try to provide any here.

In our following calculations, we will assume the above hypothesis 2 on the preceding page which also implies $\forall i \in \{1, ..., N_x\}, \forall t \in [0, \Delta t],\ \eta_i(t) = q_i(t)$.

5.2.4. *Cell boundary crossing event*

Cell boundary crossing event leads to a special treatment in the general case as it implies taking into account the term $Z^{-1}(x,t)V\omega\nabla Z(x,t)$. Due to the spatial discretization hypothesis 1, the term becomes $Z_i^{-1}(t)V\omega\nabla Z_i(t)$. Consequently, the term is non zero only when crossing the interface between two cells. The explaination is detailed in annexe B. The consequence is that each MC particle has its weight w_p multiplied by the ratios (29) when not colliding ($[0,t]$), depending on whether it changes of cell or not

$$\begin{aligned} &\text{if} \quad \{\exists t_l \in [0,t] \,|\, s \in [0,t_l] \Rightarrow x_p \in \mathcal{D}_i \text{ and } s \in [t_l,t] \Rightarrow x_p \in \mathcal{D}_j\} \\ &\quad \text{then} \quad w_p(0) = w_p(t)\frac{z_i(0)}{z_i(t_l)}\frac{z_j(t_l)}{z_j(t)}, \\ &\text{else} \\ &\quad \text{then} \quad \forall s \in [0,t], x_p \in \mathcal{D}_i \text{ and } w_p(0) = w_p(t)\frac{z_i(0)}{z_i(t)}. \end{aligned} \tag{29}$$

The treatment is very similar to the one used at cell crossing when using an importance sampling type variance reduction method.

5.2.5. *Second key step of the Unsplit MC scheme: resolution of a balanced gain-loss transport system*

Let us now tackle the tracking of particles within a cell $\mathcal{D}_i$. In (25), the first term in factor of f $(V\Sigma_t(\eta(x,t) - q(x,t)))$ is zero due to hypothesis 2. The second term $(Z_i^{-1}(t)V\omega\nabla Z_i(t))$ is zero due to hypothesis 1. It only remains to address the local MC resolution in each cell $\mathcal{D}_i$ of the following system:

$$\begin{cases} \partial_t f(x,t,\omega) + V\omega\nabla f(x,t,\omega) + V\Lambda_s(Z_i(t),\eta_i(t))f(x,t,\omega) &= V\Lambda_s(Z_i(t),\eta_i(t))\displaystyle\int P_s(Z_i(t),\eta_i(t),\omega',\omega)f(x,t,\omega')\,\mathrm{d}\omega', \\ \partial_t z_i(t) = -V\Sigma_a(\eta_i(t))z_i(t) \quad \text{with} \quad z_i(0) = \frac{1}{|\mathcal{D}_i|}\displaystyle\int_{\mathcal{D}_i}\int U^0(x,\omega')\,\mathrm{d}\omega'\,\mathrm{d}x, \\ \partial_t \eta_i(t) = V\Sigma_R(\eta_i(t))z_i(t) \quad \text{with} \quad \eta_i(0) = \frac{1}{|\mathcal{D}_i|}\displaystyle\int_{\mathcal{D}_i}\eta^0(x)\,\mathrm{d}x. \end{cases} \tag{30}$$

Our aim is now to describe the resolution of system (30) with the UMC scheme we already briefly described in the previous sections in simpler configurations. Let us now suppose we have access to the time evolution of $\Lambda_s(t) = \Lambda_s(Z_i(t),\eta_i(t)), M_s(t,\omega,\omega') = P_s(Z_i(t),\eta_i(t),\omega',\omega)$ of general terms $\lambda_s^g(t), \lambda_s^{g',g}(t,\omega',\omega)$, obtained analytically (as in section 3 on page 8) or from a solver (as in section 4 on page 14), we then have to solve a *transport equation with balanced gain-loss* which, for a given group g, resumes to:

$$\partial_t f_g(x,t,\omega) + v_g\omega\partial_x f_g(x,t,\omega) + v_g\lambda_s^g(t)f_g(x,t,\omega) = v_g\lambda_s^g(t)\sum_{g'=0}^{G}\int \lambda_s^{g',g}(t,\omega',\omega)f_{g'}(x,t,\omega')\,\mathrm{d}\omega'. \tag{31}$$

Now, on each group characteristic, we get:

$$\partial_s f_g(x+v_g\omega s,s,\omega) + v_g\lambda_s^g(s)f_g(x+v_g\omega s,s,\omega) = v_g\lambda_s^g(s)\sum_{g'=0}^{G}\int v_g\lambda_s^{g',g}(s,\omega',\omega)f_{g'}(x+v_g\omega s,s,\omega')\,\mathrm{d}\omega'.$$

Multiplying both sides by $e^{\int_0^s v_g\lambda_g(\alpha)\,\mathrm{d}\alpha}$ we then get

$$\partial_s[f_g(x+v_g\omega s,s,\omega)e^{\int_0^s v_g\lambda_g(\alpha)\,\mathrm{d}\alpha}] = v_g\lambda_s^g(s)\sum_{g'=0}^{G}\lambda_s^{g',g}(s,\omega',\omega)e^{\int_0^s v_g\lambda_g(\alpha)\,\mathrm{d}\alpha}\int f_{g'}(x+v_g\omega s,s,\omega')\,\mathrm{d}\omega'.$$

We integrate with respect to time the above expression between 0 and t and we obtain

$$f_g(x+v_g\omega t,t,\omega) = f_g^0(x,\omega)e^{-\int_0^t v_g\lambda_g(\alpha)\,\mathrm{d}\alpha} + \int_0^t v_g\lambda_s^g(s)\int\sum_{g'=0}^{G}\lambda_s^{g',g}(s,\omega',\omega)e^{-\int_s^t v_g\lambda_g(\alpha)\,\mathrm{d}\alpha}f_{g'}(x+v_g\omega s,s,\omega')\,\mathrm{d}\omega'\,\mathrm{d}s.$$

Let us introduce for the group g: $T_g(s,t) = v_g\lambda_g(s)e^{-\int_s^t v_g\lambda_g(\alpha)\,\mathrm{d}\alpha}$. We have

$$f_g(x,t,\omega) = \int \left[f_g^0(x - v_g\omega t, \omega)\mathbf{1}_{[t,\infty[}(s) + \int \sum_{g'=0}^{G} \lambda_s^{g',g}(t-s,\omega',\omega)\,\mathrm{d}\omega' f_{g'}(x - v_g\omega s, t-s, \omega')\mathbf{1}_{[0,t]}(s) \right] T_g(s,t)\,\mathrm{d}s. \tag{32}$$

It remains now to identify probability density functions for the sampling of inner group and of inner angle in expression (32). This will enable writing (32) as an expectation so that we can apply a MC resolution on it. We recall the samplings for the MC resolution are not unique (see appendix A.2 and A.3 where two sets of samplings are defined in order to solve the same transport equation), we here only suggest one set. In order to exhibit the different pdf for the different samplings of random variable, let us introduce,

$$\begin{aligned} \lambda_s^{g',g}(s) &= \int \lambda_s^{g',g}(s,\omega',\omega)\,\mathrm{d}\omega' \qquad \text{and} \quad F_{g',g}(s,\omega',\omega) = \frac{\lambda_s^{g',g}(s,\omega',\omega)}{\sum_{h=0}^{G}\lambda_s^{h,g}(s)}, \\ \forall\{g,g',s,\omega,\omega'\}, \qquad & \\ \Gamma_s^{g',g}(s,\omega) &= \int F_{g',g}(s,\omega',\omega)\,\mathrm{d}\omega', \quad \text{and} \quad \gamma_s^{g',g}(s,\omega',\omega) = \frac{F_{g',g}(s,\omega',\omega)}{\Gamma_s^{g',g}(s,\omega)}. \end{aligned} \tag{33}$$

Then by definition we have $\sum_{g'=0}^{G}\Gamma_s^{g',g}(s,\omega) = 1, \forall\{g,s,\omega\}$ and $\int \gamma_s^{g',g}(s,\omega',\omega)\,\mathrm{d}\omega' = 1, \forall\{g',g,s,\omega\}$. With the above notations, (32) becomes

$$f_g(x,t,\omega) = \int \begin{bmatrix} + & f_g^0(x - v_g\omega t, \omega) & \mathbf{1}_{[t,\infty[}(s) \\ + \int \sum_{g'=0}^{G} \Gamma_s^{g',g}(t-s,\omega)\gamma_s^{g',g}(t-s,\omega',\omega)\,\mathrm{d}\omega' & f_{g'}(x - v_g\omega s, t-s, \omega') & \mathbf{1}_{[0,t]}(s) \end{bmatrix} T_g(s,t)\,\mathrm{d}s. \tag{34}$$

Let introduce $\mathcal{U}_\mathcal{S}$ an uniform random variable on $[0,1]$. We have for the interaction time

$$\mathcal{U}_\mathcal{S} = \int_0^\mathcal{S} T_g(s,t)\,\mathrm{d}s = \int_0^\mathcal{S} v_g\lambda_g(s)e^{-\int_s^t v_g\lambda_g(\alpha)\,\mathrm{d}\alpha}\,\mathrm{d}s \text{ leading to } -\ln(\mathcal{U}_\mathcal{S}) = \int_{t-\mathcal{S}}^t v_g\lambda_g(s)\,\mathrm{d}s, \tag{35}$$

and in practice it will need an ODE resolution and it will consequently be sampled up to a chosen accuracy (ε_{acc}) as in section 4 on page 14. When a MC particle reaches the interaction time $\mathcal{S}$, it will change group and angle: thanks to the introduction of $\Gamma_s^{g',g}$ and $\gamma_s^{g',g}$ in the expressions above, the inner group is sampled and the inner angle is sampled conditionnally to the inner group. With the application of hypothesis 2 on page 24, we introduce two more uniform random variables on $[0,1]$, $\mathcal{U}_\mathcal{G}$,$\mathcal{U}_{W'}$ which satisfy

$$\mathcal{G} = \min\left\{ h \in \{1,...,G\} \,\middle|\, \mathcal{U}_\mathcal{G} < \frac{\sum_{g'=0}^{h}\Gamma_s^{g',g}(t-\mathcal{S},\omega)}{\sum_{g'=0}^{G}\Gamma_s^{g',g}(t-\mathcal{S},\omega)} \right\} \text{ and once } \mathcal{G} \text{ sampled we have } \mathcal{U}_{W'} = \int_{-\infty}^{W'} \gamma_s^{\mathcal{G},g}(t-\mathcal{S},\omega',\omega)\,\mathrm{d}\omega'. \tag{36}$$

Now that the random variables are introduced, we can rewrite the transport equation as an expectation we can approximate thanks to a MC method

$$f_g(x,t,\omega) = \mathbb{E}\left[\mathbf{1}_{[t,\infty]}(\mathcal{S})f_g^0(x - v_g\omega t,\omega) + \mathbf{1}_{[0,t]}(\mathcal{S})\delta_{g'}(\mathcal{G})f_{g'}(x - v_g\omega\mathcal{S}, t-\mathcal{S}, W')\right], \tag{37}$$

which can also be rewritten in a recursive way in order to apply a MC solver (as in appendix A.3 for example).

Remark 1 *We remind the pdf and the laws introduced in this part are in an adjoint form, we refer to [19] for the reader to transform them in a direct form.*

5.3. *The non-analog/flight path MC scheme as a particular case of the presented methodology*

It is worth noting that the multi-group extension of the non-analog scheme presented in appendix A.3 is a particular case of the methodology we presented in previous section. Indeed, it corresponds to a particular choice of ODE/change of

variable: instead of performing the change of variable (23), the well known flight path MC scheme performs the following one

$$\begin{cases} \partial_t z_i(t) = -diag_{g\in\{1,\dots,G\}}(v_g(\sigma_t^g - \sigma_s^g))\eta_i(t)z_i(t), & \text{with} \quad z_i(0) = \frac{1}{|\mathcal{D}_i|}\displaystyle\int_{\mathcal{D}_i}\int U(x,0,\omega')\,\mathrm{d}\omega'\,\mathrm{d}x, \\ \partial_t \eta_i(t) = 0, & \text{with} \quad \eta_i(0) = \frac{1}{|\mathcal{D}_i|}\displaystyle\int_{\mathcal{D}_i}\eta(0,x)\,\mathrm{d}x. \end{cases} \tag{38}$$

Such change of variable does not need an ODE solver, it leads to explicit formula (as in section 3 on page 8) as η does not vary with time, so that we have $\forall g \in \{1,...,G\}$ $z_i(t) = z_i(t^n)\ \frac{e^{v\sigma_a\eta_i t}}{e^{v\sigma_a\eta_i t^n}}$ and we recover the classical weight modification of the scheme presented in appendix A.3 which becomes more generally

$$\begin{aligned} &\text{if} \quad \{\exists t_l \in [0,t]\,|\,s\in[0,t_l] \Rightarrow x_p \in \mathcal{D}_i \text{ and } s\in[t_l,t]\Rightarrow x_p\in\mathcal{D}_j\} \\ &\qquad \text{then} \quad \frac{z_i(0)}{z_i(t_l)}\frac{z_j(t_l)}{z_j(t)} = e^{-v\sigma_a\eta_i t_l}e^{-v\sigma_a\eta_j(t-t_l)}, \\ &\text{else} \\ &\qquad \text{then} \quad \forall s\in[0,t], x_p\in\mathcal{D}_i \text{ and } \frac{z_i(0)}{z_i(t)} = e^{-v\sigma_a\eta_i t}, \end{aligned} \tag{39}$$

depending on whether the MC particle crosses a cell or not. We consider the UMC methodology generalizes the flight path/non-analog scheme of appendix A.3 in the sense that the latter corresponds to an approximation in the change of variable (26).

5.4. *A quick sum-up for the application of the UMC scheme to system* (21)

Finally, to sum up the UMC methodology in few points, we would say that:

- It implies performing a change of variable (23) in order to weaken the coupling and get a balanced gain-loss transport in system (22).
- This change of variable corresponds to a generalization of the classical schemes like the well-known multi-group non-analog/flight path scheme (the change of variable (38) being an approximation of (23)).
- The transport counterpart of (22), once the change of variable performed, becomes a balanced *gain-loss* transport equation (30) with time dependent characteristics within a cell. The samplings of the interaction time, the inner group and angle are consequently more complex but can be handled.
- The only two discretization hypothesis applied to describe the UMC methodology are hypothesis 1 on page 24 and hypothesis 2 on page 24.

In this section, we described the UMC methodology, explained why the schemes presented in sections 3 and 4 are particular cases of it and how it generalizes the classical ones. Let us now present some numerical results emphasizing the fact that even with energy/velocity dependences, the properties with respect to instabilities (point (i) of section 2.8 on page 8) and sensitiveness with respect to time discretization are still holding.

6. Application of the UMC scheme to the problem 2g2r-h in the 2 groups - 2 materials case

In this section, we apply the UMC solver to a new homogeneous (h) test-problem with energy/velocity dependent transport equation, 2 groups (2g), a 2 materials vector (2r) $\eta = (\eta_A, \eta_B)^t$ (inducing a 4×2 reaction matrix). So, with $g\in\{1,2\}$ and $r\in\{1,2\}$, we have $\sigma_R^{r,g}$ in which the exponent r is for the reaction and the exponant g is for the group. We denote by

$$\Sigma_R^g = \begin{pmatrix} -\sigma_R^{0,g} & +\sigma_R^{1,g} \\ +\sigma_R^{0,g} & -\sigma_R^{1,g} \end{pmatrix} = P_g\Lambda_R^g P_g^{-1} = P_g \begin{pmatrix} 0 & 0 \\ 0 & -\sigma_R^{0,g} - \sigma_R^{1,g} \end{pmatrix} P_g^{-1}, \tag{40}$$

where Λ_R^g is the diagonal matrix of Σ_R^g.

$$\partial_t\eta = \Sigma_R^0(\eta)u_0 + \Sigma_R^1(\eta)u_1 \tag{41}$$

The matrices Σ_R^0 and Σ_R^1 are mainly introduced in this section is order to justify that in general they are not diagonalizable in the same basis (P_0 and P_1 are not proportional) and the construction on an ODE of unknown V in no more applicable as it was in section 4.3 on page 19.

(U_0^0, U_1^0)	(η_A^0, η_B^0)	(v_0, v_1)	$\sigma_t^{i,g}$, $i \in \{A, B\}$, $g \in \{0, 1\}$	Σ_s^A Σ_s^B	Σ_R^0 Σ_R^1	left BC	right BC
$(0.50, 0.50)$	$(0.40, 0.60)$	$(1.00, 2.00)$	1.00	$\begin{pmatrix} 0.80 & 0.30 \\ 0.20 & 0.06 \end{pmatrix}$ $\begin{pmatrix} 0.20 & 0.50 \\ 0.10 & 0.90 \end{pmatrix}$	$\begin{pmatrix} 0.00 & 0.00 \\ 0.00 & 0.00 \end{pmatrix}$ $\begin{pmatrix} -1.00 & 1.00 \\ 1.00 & -1.00 \end{pmatrix}$	specular	2g2r-h : specular 2g2r-nh : free

Fig. 18. Parameters for the tests 2g2r-h and 2g2r-nh only differing through domain right boundary condition.

We insist on the fact that we do not intend to build physical constants with problem 2g2r-h of table 18 but relevant ones in order to obtain a stiff problem for which the classical scheme lacks efficiency: for example, the chosen scattering matrix for each material cannot represent a scattering matrix in a neutron problem as it allows scattering from the lower group to the higher one. Nevertheless, we detail the behavior of the solutions with respect to time for the different quantities on a homogeneous problem: first, globally, the test-problem is absorbing in term of particles, whatever its group, this is emphasized by the fact that $\forall g, g', \sigma_s^{A,g',g} < \sigma_t^{A,g}$ and $\forall g, g', \sigma_s^{B,g',g} < \sigma_t^{B,g}$. There are no reaction for material A whereas there are strong ones for material B in each group leading to a fast conversion of material A into material B in the early times of the simulation. Reference curves are displayed with respect to time for each quantities in fig. 19 on the next page.

In the following, we solve the above problem with the classical scheme and the new one we presented in the above section. We remind that in the following, the *classical* scheme will denote a split scheme between the transport and the Bateman phases, with the MC scheme of appendix A.3 in order to solve the transport scheme, and the fixed-up explicit Euler scheme for the Bateman phase. Fig. 19 on the following page also presents the results obtained with the classical scheme for two time-steps $\Delta t = 2$ and $\Delta t = 1$ and $N_{MC} = 5000$. For this test problem we kept N_{MC} low in order to show that if instabilities with respect to time are easy to identify on the group particle densities U_0, U_1 (red $\times$ in top figures), this is less obvious for $\Delta t = 1$ in blue $+$ on the same figures due to MC noise which cannot be distinguished from spurious oscillations. However, they are clearly present for both time-step values in time evolution of the materials densities displayed in the bottom figures.

Let us now tackle the same problem with the UMC scheme we presented in section 5 on page 21.

Fig. 20 on the next page presents the results obtained with the UMC scheme in an even coarser condition than in fig. 19 on the following page as we take $N_{MC} = 5000$ but $\Delta t = 5$. The figure testifies the UMC scheme prevents the development of oscillations (point (i) of section 2.8 on page 8) and ensures a good agreement with the reference solution.

We now consider the same test problem as above but with vacuum boundary condition, i.e. problem 2g2r-nh of table 18, on the right hand side boundary ($x = 1$) of the simulation domain $\mathcal{D} = [0, 1]$.

Fig. 21 on page 30 presents the time evolution of the different quantities for the classical scheme (left column) and the new MC scheme (right column) in exactly the same conditions, $N_{MC} = 100000$ and several time-steps values. The figure allows verifying a weak dependence with respect to the time discretization (point (iii) of section 2.8 on page 8) of the solution for the UMC scheme especially on the materials evolution $\eta_A(t), \eta_B(t)$ in opposition to the classical scheme. The scales are the same for both schemes in order to appreciate the differences between them.

7. Conclusion: summary of the paper, limitations and future work

To close this paper, we would like to come back on its main aspects and on future work for the UMC scheme.

This paper introduces a new UMC scheme for the coupling of the linear Boltzmann equation and the Bateman system under very general conditions. Still, the paper lacks a section describing how we deal with sources in the transport equation within the UMC methodology (for example, for applications in neutronics, with Bateman equations as treated here, only prompt neutrons are considered whereas it is a well-known fact that delayed ones are mandatory).

First, in section 3 on page 8, on a simplified configuration (monokinetic+mono-material), we showed how plugging the analytical solution of section 2.1 on page 3 in a MC scheme with time dependent characteristics allowed a gain on the three weak points (i), (ii) and (iii) put forward in section 2.8 on page 8. Thanks to numerical experimentations, we verified that the UMC scheme prevented the occurrence of numerical instabilities when they used to appear with a classical split scheme. We also verified that the obtained approximations were less sensitive to the chosen time discretization. Secondly, the results of section 3 on page 8 being encouraging, we extended the methodology to the monokinetic case with non scalar reaction matrix (non degenerate Bateman equations). In this context, no analytical solution was available even for the homogeneous problem. We relied on a numerical scheme in order to solve a reduced model on-the-fly (homogeneous

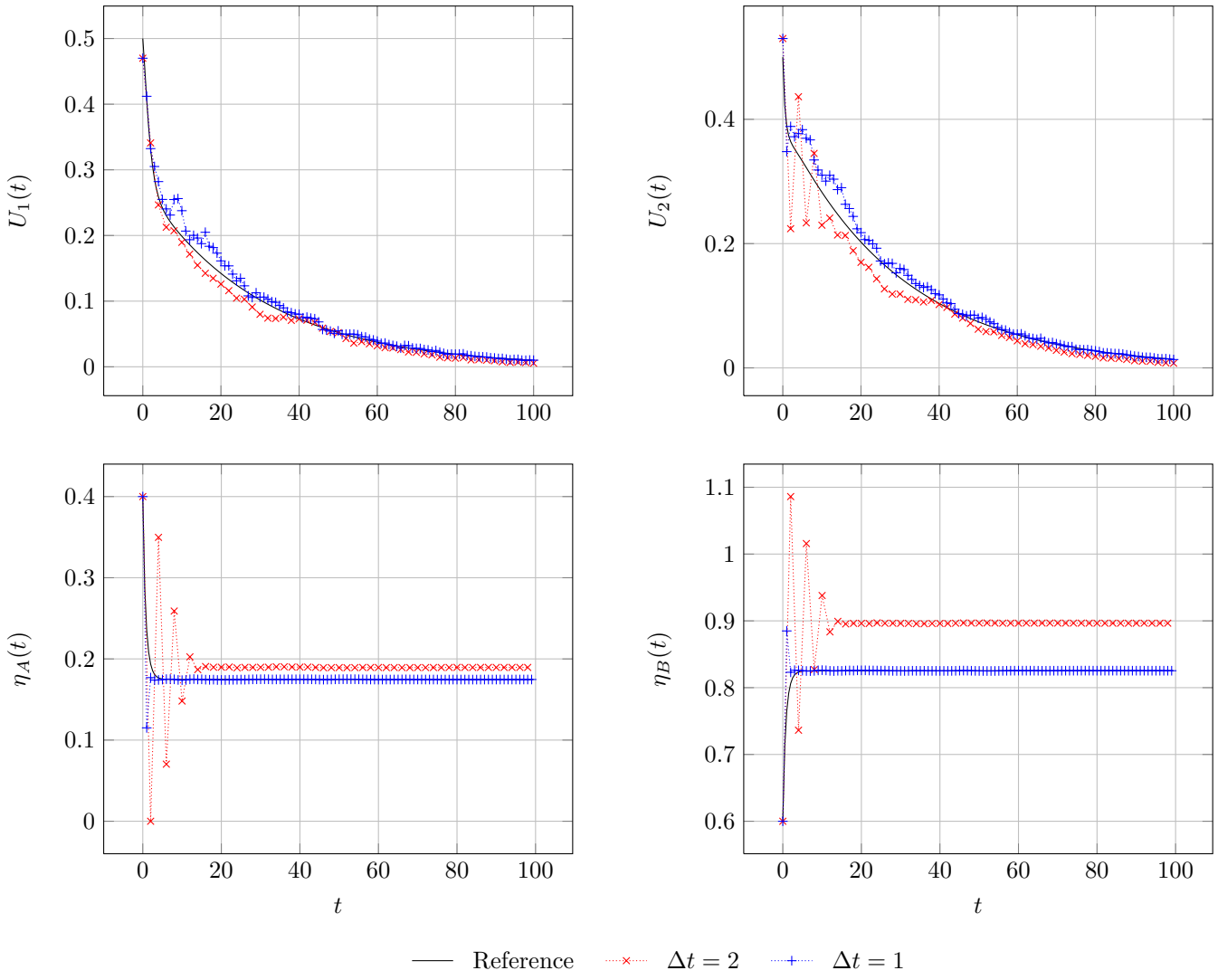

Fig. 19. Time evolutions of U_1, U_0 (top) and η_A, η_B (bottom) with the classical scheme with 2 time discretizations $\Delta t = 2$ and $\Delta t = 1$.

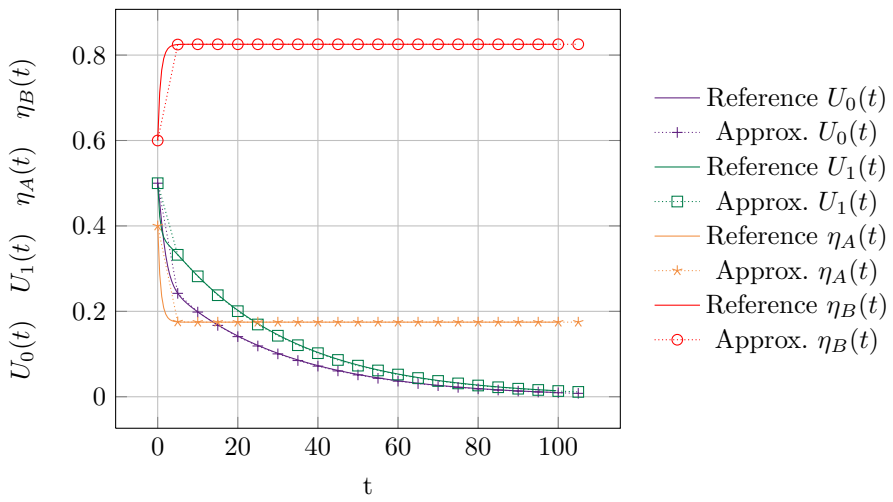

Fig. 20. Time evolutions of the computed $U_0(t), U_1(t), \eta_A(t), \eta_B(t)$ with the new solver for the resolution of the problem of section 4.3 on page 19 for $\Delta t = 5$.

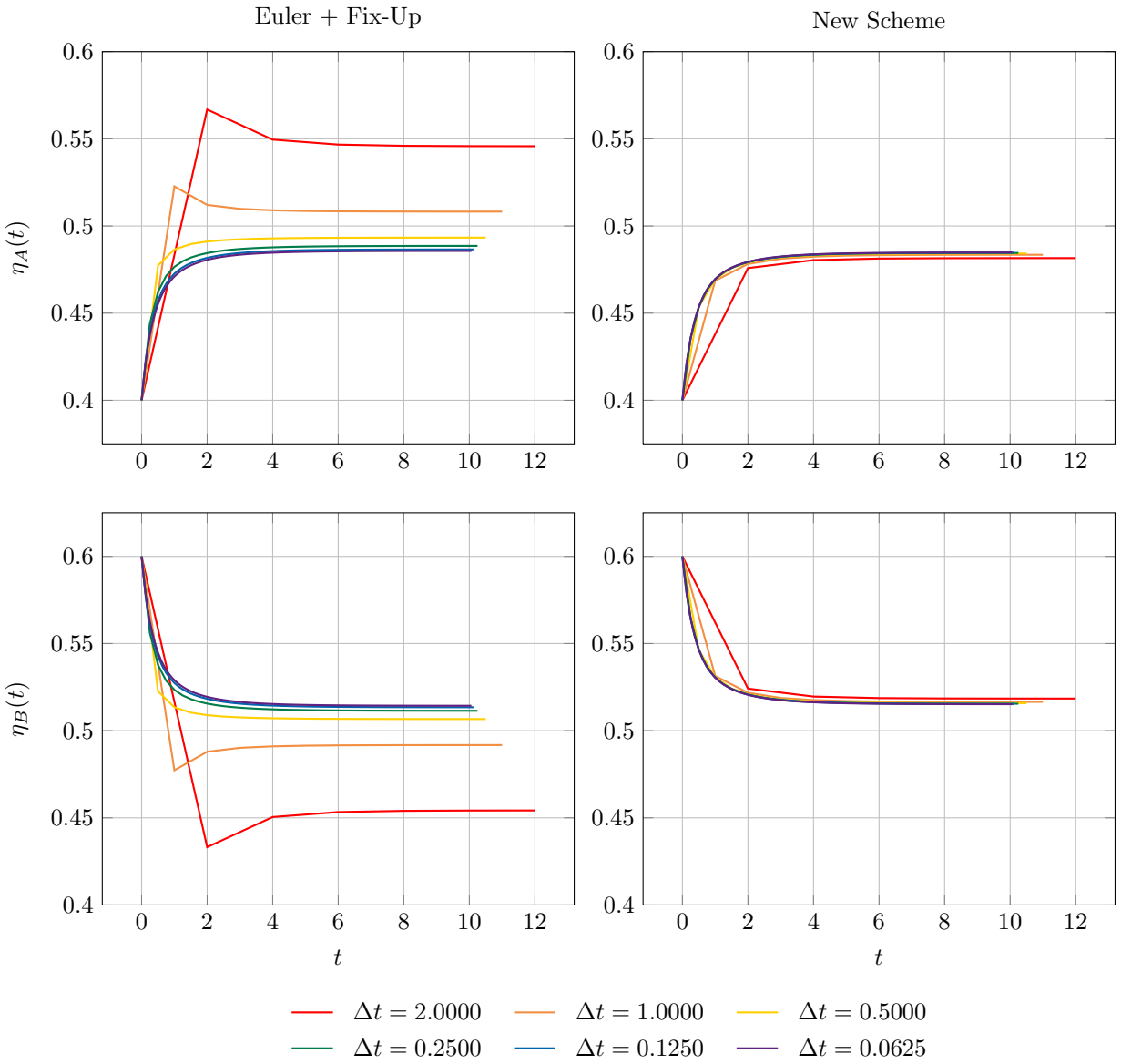

Fig. 21. Time evolution of $\eta_A(t)$ and $\eta_B(t)$ for the configuration of section 6 on page 27 for the classical scheme (left) and the new MC scheme (right) for several time discretizations Δt and $N_{MC} = 10000$. A common scale is used for both schemes.

= integrated with respect to directions + no transport term, see (15)). This intermediary step was introduced here, before the general description of section 5 on page 21, in order to focus on the situation where no analytical solution can be plugged in the time dependent MC method. The problematic can be handled with a numerical evaluation of time evolution of the characteristics of the particles. This section details the main aspects of the UMC scheme (interaction times, weight modifications, direction changes) computed from an ODE solver. The general methodology (energy/velocity dependence+non degenerate Bateman equations) is described in section 5 on page 21. We emphasized the main idea of the UMC scheme is to perform a change of variable (see expression (23)) in order to solve a balanced gain-loss transport equation with a MC scheme (30) implying time dependent characteristics. It corresponds to a generalization of the flight path/non-analog scheme described in appendix A.3 which is intensively used in many physical applications/simulation codes. Through numerical experimentations, we verified the properties of the UMC scheme with respect to instabilities and sensitiveness to time discretization are still holding, even in more general configurations.

Now, we think physical considerations and High Performance Computing (HPC) ones are strongly correlated. Indeed, in section 5 on page 21, the change of variable we suggest in the UMC methodology needs the numerical resolution of system of ODE of size $G + M$ where G is the number of groups and M is the number of considered materials in the simulations. The size of the matrix obtained from linearization of the second part of the ODE can be very important (see applications in neutronics for example [3]). In fact, thanks to HPC accelerations, we hope the UMC scheme will

be computationally efficient: the *on the fly* resolution of an ODE with MC particles evolving in the geometry can benefit GPGPU accelerations which are more and more common (see [2] for applications to hydrodynamics coupled to a quadratic ODE for fusion reactions for example). The important amount of data loaded for the ODE system is associated to important amount of computations (more than the classical schemes), thus the method may be less sensitive to memory localization which is a complex issue in HPC [9]. Moreover, particles in a cell could be buffered to benefit the ODE resolution. Finally, the independence between MC particles still holds with the UMC scheme. Consequently, the new scheme can still benefit replication domain parallelism (see [9]) which is common for MC scheme. The capability of the UMC scheme to deal with bigger time steps could even mean that we may be able to reduce the frequency of parallel reductions contention points (see [9]).

We finally would like to hint at what we think are complementary points for the discussion: regarding the change of variable at the basis of the method, it implies the resolution of an ODE which we solved with a very simple explicit Euler scheme. More efficient ones could have been used, especially if asymptotic preserving/well balanced properties are required. We did not want to complexify the paper with such considerations but we put forward the UMC scheme can benefit every numerical advances in term of ODE resolution. Note also that we chose to *solve* the ODE for the change of variable whereas we could have approximated it: this was suggested in section 3 on page 8 with the example of the second order development of the interaction time with respect to $\sigma_R \sim 0$ (see expression (9)). In the same way, in the case of the non degenerate Bateman equation, for example, we could have *approximated* formula (15) for which we do not have analytical solution rather than *solve* it: indeed, assuming $(\lambda_j \sim 0)_{j\in\{1,\dots,N\}}$ and performing a development up to order k ($\mathcal{O}(\lambda_j^k)$) leads to an approximated ODE which, in this particular case, *can be solved analytically* and consequently we would not need a solver anymore for the different samplings. Obviously, solving the ODE without further approximations also allows having a reference: with this (eventually costly) reference we will be able to test the relevance of any chosen approximation. Such kind of considerations will be studied in future works in order to reduce the cost of the scheme but will certainly trade computational efficiency with more sensitiveness with respect to time discretization. We built the method so that it is less sensitive to time-step, and verified it experimentally. We will perform the complete numerical analysis (conditions for the properties to hold etc.) in further publications too. Regarding energy/velocity dependences, we only treated the multi-group approach and only hinted at the punctual one. We think the UMC solver is still applicable in this context, but the change of variable it implies will need a different strategy for its resolution (Monte-Carlo for example). Finally, we insist on the fact that the UMC scheme does not treat pure 'transport' effects as the scheme presented in [7] does. Typically, if the transport (spatial effects) becomes preponderant in the change rate of the particle/material density (i.e. due to the $v\omega\nabla u(x,t,v,\omega)$ operator), the UMC scheme will still need the same time-step as the classical split ones in order to be accurate. Nonetheless, in every other situations, we think UMC scheme allows interesting gains.

8. Acknowledgements

The authors would like to thank David Dureau and Cédric Enaux for some valuable discussions about respectively High Performance Computing and Numerical Analysis.

Appendix A. Monte-Carlo solver in a nutshell

In this section, we present two different and widespread MC schemes for the resolution of the transport equation with constant characteristics [25, 15, 16]. Note that for the purpose of the paper, it is enough here describing the schemes in the monokinetic case without loss of generalities.

In this section, we briefly detail how a MC solver is built from rewriting the transport equation into an integral form.

A.1. *Integral form of the transport equation*

The monokinetic transport equation with constant characteristics $(\sigma_\alpha)_{\alpha\in\{s,t\}}$ is given by

$$\partial_t u(x,t,\omega) + v\omega\nabla u(x,t,\omega) + v\sigma_t u(x,t,\omega) = \int v\sigma_s P_s(\omega',\omega)u(x,t,\omega')\,\mathrm{d}\omega',$$

where $P_s(\omega',\omega)$ is the probability for a particle p having direction ω' to get out of an interaction with direction ω. Let us now rewrite (A.1) in a recursive integral form: for this, we apply the characteristic method and multiply (A.1) by $\exp(v\sigma_t s)$ so that the transport equation becomes

$$\partial_s \left[u(x+v\omega s,s,\omega)e^{v\sigma_t s}\right] = \int v\sigma_s P_s(\omega',\omega)u(x+v\omega s,s,\omega')e^{v\sigma_t s}\,\mathrm{d}\omega'.$$

Integrating between 0 and t leads to

$$u(x+v\omega t,t,\omega) = u_0(x,\omega)e^{-v\sigma_t t} + \int_0^t \int v\sigma_s P_s(\omega',\omega)u(x+v\omega s,s,\omega')e^{-v\sigma_t(t-s)}\,\mathrm{d}\omega'\,\mathrm{d}s. \tag{A.1}$$

and noticing that

$$e^{-v\sigma_t t} = \int_t^\infty v\sigma_t e^{-v\sigma_t s}\,\mathrm{d}s,$$

leads to (together with a variable change $t-s=m$ in which we keep the notation s)

$$u(x+v\omega t,t,\omega) = \int \mathbf{1}_{[t,\infty[}(s)u_0(x,\omega)v\sigma_t e^{-v\sigma_t s}\,\mathrm{d}s + \int\int \left\{ \begin{array}{l} \frac{v\sigma_s}{v\sigma_t}u(x+v(t-s)\omega,t-s,\omega')\times \\ P_s(\omega',\omega)\times \mathbf{1}_{[0,t]}(s)v\sigma_t e^{-v\sigma_t s} \end{array} \right\} \mathrm{d}\omega'\,\mathrm{d}s, \tag{A.2}$$

in which, in the last term of (A.2), we separated the integrand from the weighting integration fonctions. With (A.2), the transport equation is written in a recursive integral form.

A.2. *MC resolution of the transport equation by a semi-analog scheme*

MC methods are based on the exploitation of the previous integral form of the transport equation. It consists in the introduction of random variables and rewriting the integral form of the transport equation as an expectation over the latter introduced random variables: let's denote by $\mathcal{S} \sim \mathcal{E}(v\sigma_t)$ and $W' \sim P_s(\omega,W')$ two random variables, we can rewrite equation (A.2) in term of a recursive expectation

$$u(x,t,\omega) = \mathbb{E}\left[\mathbf{1}_{[t,\infty[}(\mathcal{S})u_0(x-v\omega t,\omega) + \mathbf{1}_{[0,t]}(\mathcal{S})\frac{v\sigma_s}{v\sigma_t}u(x-v\mathcal{S}\omega,t-\mathcal{S},W')\right]. \tag{A.3}$$

In the previous integral expression, we recognize what is commonly called [15, 25, 16]

- the 'census event': if $\mathcal{S} > t$ which corresponds to a transport of the particle along $v\omega t$,
- the 'scattering event': if $\mathcal{S} < t$ which corresponds to a transport of the particle along $v\omega\mathcal{S}$, a change of direction W' of the particle and a weight of the particle multiplied by $\frac{\sigma_s}{\sigma_t}$ both at the interaction point $x - v\omega\mathcal{S}$.

The MC resolution of (A.3) consists in formulating the expectation as a mean over a finite number N_{MC} of realizations of the previously introduced random variables, while eliminating the recursive implication of u in (A.3) by sorting by number of scattering events: for this, we introduce the notations δ_j^p for a particle p having exactly j interactions in the time interval $[0,t]$

$$\delta_j^p = \mathbf{1}_{\left\{\sum_{l=0}^{j}\mathcal{S}_l^p < t\right\}} \times \mathbf{1}_{\left\{\sum_{l=0}^{j+1}\mathcal{S}_l^p \geq t\right\}},$$

where $(\mathcal{S}_l^p)_{l\in\{0,\ldots,j+1\}}$ are independent identically distributed random variables $\sim \mathcal{E}(v\sigma_t)$. We also introduce the process

$$X_j^p = v\omega(t-\mathcal{S}_j^p) + \sum_{l=1}^{j-1} vW_l^p\mathcal{S}_l^p,$$

where $W_l^p \sim P_s(W_l^p, W_{l-1}^p)$, and where respectively ω, W_l^p are the directions of the particles between times $\mathcal{S}_j^p$ and t, $\mathcal{S}_l^p$ and $\mathcal{S}_{l-1}^p$. Finally, the MC resolution of equation (A.2) by a semi-analog scheme consists in following the N_{MC} particles on the resolution domain through the jump processe X_j^ps

$$\begin{aligned} u(x,t,\omega) &= \sum_{p=1}^{\infty}\sum_{j=0}^{\infty}\delta_j^p \left(\tfrac{\sigma_s}{\sigma_t}\right)^j u_0(x-X_j^p,W_0^p), \\ &\approx \sum_{p=1}^{N_{MC}}\sum_{j=0}^{\infty}\delta_j^p \left(\tfrac{\sigma_s}{\sigma_t}\right)^j u_0(x-X_j^p,W_0^p). \end{aligned} \tag{A.4}$$

The second sum in the second line of (A.7) is infinite but having a finite number of particles N_{MC}, the number of interactions encountered by this population of MC particles is also finite.

The MC solver, in order to compute the density of physical particles at x, t, ω consists in following N_{MC} MC particles from the initial condition u_0 along the paths of the jump process X_j^p with modification of the weights of the MC particles modeling the absorption or multiplication of particles due to material interactions (term $(\frac{\sigma_s}{\sigma_t})^j$).

The MC scheme presented previously in A.2 equation (A.7) will be denoted by 'semi-analog scheme' in the whole paper: an analog scheme would mimic the physics and, for example kill an absorbed particle, see [15, 25, 16], whereas in the semi-analog scheme presented above a MC particle p does not represent one physical particle but the mean of a population of particles.

The 'semi-analog' denomination, in opposition to a non-analog one (see section A.3), comes from the fact that the scheme can not analytically solve the homogeneous form of (A.1) in the unknown $U(t) = \int u(t,\omega)\,\mathrm{d}\omega$

$$\partial_t \int u(t,\omega)\,\mathrm{d}\omega = -v\sigma_t \int u(t,\omega)\,\mathrm{d}\omega + v\sigma_s \int u(t,\omega')\,\mathrm{d}\omega',$$

having for solution $U(t) = U_0 e^{-v\sigma_a t}$. Indeed, the variance of the built process, in the limit of an infinite number of particles is given by

$$\mathrm{var}(t) = U_0^2 \left(e^{\dfrac{(v\sigma_s)^2 - (v\sigma_t)^2}{(v\sigma_t)} t} - e^{2(v\sigma_s - v\sigma_t)t} \right),$$

and is in general non zero (except for non absorbing media, i.e. if $\sigma_s \neq \sigma_t$).

A.3. *MC resolution of the transport equation by a non-analog scheme*

The non-analog scheme is based on a slightly different writing of the integral form of the transport equation. In order to present the main feature of the non-analog MC scheme, we start with the same monokinetic transport with constant coefficients (A.1) but the idea here is to apply different variable changes. Let us introduce $\sigma_t = \sigma_a + \sigma_s$. Then by noticing that

$$e^{-v\sigma_\alpha t} = \int_t^\infty v\sigma_\alpha e^{-v\sigma_\alpha s}\,\mathrm{d}s, \alpha \in \{s, a\},$$

(A.1) becomes

$$u(x+v\omega t, t, \omega) = \int \mathbf{1}_{[t,\infty[}(s) u_0(x,\omega) e^{-v\sigma_a t} v\sigma_s e^{-v\sigma_s s}\,\mathrm{d}s + \int\int \left\{ \begin{array}{l} e^{-v\sigma_a s} u(x+v(t-s)\omega, t-s, \omega') \times \\ P_s(\omega', \omega) \times \mathbf{1}_{[0,t]}(s) v\sigma_s e^{-v\sigma_s s} \end{array} \right\} \mathrm{d}\omega'\,\mathrm{d}s, \quad \text{(A.5)}$$

with, in the last term of (A.5), we separated the integrand from the weighting integration functions.

Let's now introduce $\mathcal{S} \sim \mathcal{E}(v\sigma_s)$ and $W' \sim P_s(\omega, W')$, we can rewrite the latter equation in term of a recursive expectation over the previous random variables

$$u(x,t,\omega) = \mathbb{E}\left[\mathbf{1}_{[t,\infty[}(\mathcal{S}) u_0(x - v\omega t, \omega) e^{-v\sigma_a t} + \mathbf{1}_{[0,t]}(\mathcal{S}) u(x - v\mathcal{S}\omega, t - \mathcal{S}, W') e^{-v\sigma_a \mathcal{S}} \right],$$

which we rewrite as

$$u(x,t,\omega) = \mathbb{E}\left[\mathbf{1}_{[t,\infty[}(\mathcal{S}) \frac{e^{-v\sigma_a t}}{e^{-v\sigma_a 0}} u_0(x - v\omega t, \omega) + \mathbf{1}_{[0,t]}(\mathcal{S}) \frac{e^{-v\sigma_a t}}{e^{-v\sigma_a (t-\mathcal{S})}} u(x - v\mathcal{S}\omega, t - \mathcal{S}, W') \right]. \quad \text{(A.6)}$$

In the previous integral expression, we recognize what is commonly called [15, 25, 16]

- the 'census event': if $\mathcal{S} > t$ which corresponds to a transport of the particle along $v\omega t$ with a change in the weight of the particle which is multiplied by $e^{-v\sigma_a t}$,
- the 'scattering event': if $\mathcal{S} < t$ which corresponds to a transport of the particle along $v\omega\mathcal{S}$, a change of direction W' of the particle and a weight of the particle multiplied by $e^{-v\sigma_a \mathcal{S}}$ both at the interaction point $x - v\omega\mathcal{S}$.

The MC resolution of (A.5) consists in formulating the expectation as a mean over a finite number N_{MC} of realizations of the previously introduced random variables, while eliminating the recursive implication of u in (A.5) by sorting by number of scattering events: for this, we introduce the notations δ_j^p for a particle p having exactly j interactions in the time interval $[0, t]$

$$\delta_j^p = \mathbf{1}_{\left\{\sum_{l=0}^{j} \mathcal{S}_l^p < t\right\}} \times \mathbf{1}_{\left\{\sum_{l=0}^{j+1} \mathcal{S}_l^p \geq t\right\}},$$

where $(\mathcal{S}_l^p)_{l \in \{0,\ldots,j+1\}}$ are independent identically distributed random variables $\sim \mathcal{E}(v\sigma_s)$. We also introduce the process

$$X_j^p = v\omega(t - \mathcal{S}_j^p) + \sum_{l=1}^{j-1} vW_l^p \mathcal{S}_l^p,$$

where $W_l^p \sim P_s(W_l^p, W_{l-1}^p)$, and where respectively ω, W_l^p are the directions of the particles between times $\mathcal{S}_j^p$ and t, $\mathcal{S}_l^p$ and $\mathcal{S}_{l-1}^p$. Finally, the MC resolution of equation (A.2) by a non-analog scheme consists in following the N_{MC} particles on the resolution domain through the jump processes X_j^p

$$\begin{aligned} u(x,t,\omega) &= \sum_{p=1}^{\infty}\sum_{j=0}^{\infty} \delta_j^p \quad e^{-v\sigma_a t} \;\; u_0(x - X_j^p, W_0^p), \\ &\approx \sum_{p=1}^{N_{MC}}\sum_{j=0}^{\infty} \delta_j^p \;\; e^{-v\sigma_a t} \;\; u_0(x - X_j^p, W_0^p). \end{aligned} \tag{A.7}$$

This scheme is non-analog in the sense it can analytically solve, (i.e. with only one particle) the homogeneous form of (A.1) in the unknown $U(t) = \int u(t,\omega)\,\mathrm{d}\omega$

$$\partial_t \int u(t,\omega)\,\mathrm{d}\omega = -v\sigma_t \int u(t,\omega)\,\mathrm{d}\omega + v\sigma_s \int u(t,\omega')\,\mathrm{d}\omega',$$

having for solution $U(t) = U_0 e^{-v\sigma_a t}$. Indeed, the variance of the built process in this case is zero whatever the number of particle used for the discretization. By definition, the non-analog scheme is more accurate than the semi-analog one. Both schemes have been introduced in this paper in order to emphasize the fact that the difficulties at stake in the discussions are independent of the MC schemes used in order to solve the transport equation. Note that MC schemes are often used in combination with variance reduction techniques: in this paper, we chose to use the most simple schemes for the sake of reproducibility of the results by a pair but we insist variance reduction methods can be applied in complement for the resolution of the transport equation.

Appendix B. Handling cell boundary crossing event

In this section, we detail how we handle the cell boundary crossing event all along the paper. In fact, the treatment is the same as the one applying when considering *importance sampling* as a variance reduction method. Consquently, the material can be considered well known amongst the MC users' community and we decided to present it only in the appendix of this paper.

In order to deal with cell boundary crossing, we need to suppose spatial dependences for the characteristics $(\sigma_\alpha)_{\alpha\in\{s,t,R\}}$. It is enough considering the monokinetic case for the purpose of this section. Consequently, we consider the following transport equation

$$\partial_t u(x,t,\omega) + v\omega\nabla u(x,t,\omega) + v\sigma_t(x,t)u(x,t,\omega) = \int v\sigma_s(x,t)P_s(x,t,\omega,\omega')u(x,t,\omega')\,\mathrm{d}\omega'. \tag{B.1}$$

First, as explain in [19], we can write the transport equation in integral form even under the previous assumptions. In the analog case, this leads to

$$u(x,t,\omega) = \int \left[\begin{array}{l} +\mathbf{1}_{[t,\infty[}(s) e^{-v\int_0^t \sigma_a^{x,t,v,\omega}(\beta)\,\mathrm{d}\beta} u_0(x - v\omega t, \omega) \\ +\mathbf{1}_{[0,t]}(s) \displaystyle\int e^{-v\int_0^s \sigma_a^{x,t,v,\omega}(\beta)\,\mathrm{d}\beta} u(x - v\omega s, t - s, \omega') P_s^{x,t,v,\omega}(s,\omega,\omega')\,\mathrm{d}\omega' \end{array}\right] \times v\sigma_s^{x,t,v,\omega}(s) e^{-v\int_0^s \sigma_s^{x,t,v,\omega}(\beta)\,\mathrm{d}\beta}\,\mathrm{d}s,$$

where the parameterization by x, t, v, ω of the characteristics has been made explicit, i.e.

$$\forall (\sigma_\alpha)_{\alpha\in\{s,t,R\}}, \sigma_\alpha^{x,t,v,\omega}(s) = \sigma_\alpha(x - v\omega s, t - s).$$

We can introduce the probability measures

$$\mathrm{d}P_{\mathcal{S}}^{x,t,v,\omega}(s) = v\sigma_s^{x,t,v,\omega}(s) e^{-v\int_0^s \sigma_s^{x,t,v,\omega}(\beta)\,\mathrm{d}\beta}\,\mathrm{d}s, \tag{B.2}$$

and

$$\mathrm{d}P_s^{x,t,v,\omega}(s,\omega,\omega') = P_s^{x,t,v,\omega}(s,\omega,\omega')\,\mathrm{d}\omega', \tag{B.3}$$

and rewrite the transport equation as an expectation over the following random variables $\mathcal{S}$ and W' such that

- $\mathcal{S} \sim P_{\mathcal{S}}^{x,t,v,\omega}(s)$, which is the probability density function of a generalized exponential law,
- $W' \sim P_s^{x,t,v,\omega}(s,\omega,\omega')$, which is the probability density function ruling angle change.

We then obtain

$$u(x,t,\omega) = \mathbb{E}\left[u_0(x-v\omega t,\omega)e^{-\int_0^t v\sigma_a^{x,t,v,\omega}(\alpha)\,\mathrm{d}\alpha}\mathbf{1}_{[t,\infty[}(\mathcal{S}) + u(x-v\omega\mathcal{S},t-\mathcal{S},W')e^{-\int_{t-\mathcal{S}}^t v\sigma_a^{x,t,v,\omega}(\alpha)\,\mathrm{d}\alpha}\mathbf{1}_{[0,t]}(\mathcal{S})\right]. \quad \text{(B.4)}$$

We defined general sampling formulas for interaction time ($P_{\mathcal{S}}^{x,t,v,\omega}$), and angular scattering ($P_s^{x,t,v,\omega}$), but also particle weight change on free flight ($e^{-\int_{t-\mathcal{S}}^t v\sigma_a^{x,t,v,\omega}(\alpha)\,\mathrm{d}\alpha}$) without any approximation nor hypothesis on material properties $(\sigma_\alpha(x,t))_{\alpha\in\{s,t,R\}}$.

The next step consists in focusing on the impact of cell boundary crossing event in the integral formulation. As we made no hypothesis on material properties we can simply introduce a discontinuity (constant characteristics within a cell with respect to space for example). Note that the correlation between space and time along a flight path, $x-v\omega t$ made explicit in the different probability law, shows that it is equivalent considering a discontinuity of $(\sigma_\alpha^{x,t,v,\omega}(s))_{\alpha\in\{s,t,R\}} = (\sigma_\alpha(x-v\omega s,s))_{\alpha\in\{s,t,R\}}$ with respect to time without loss of generality.

So let us now consider that $\exists t_l$ such that

$$\forall\alpha\in\{s,t,R\}, \sigma_\alpha^{x,t,v,\omega}(s) = \begin{cases} \sigma_{\alpha,1}^{x,t,v,\omega}(s) & \text{if } s < t_l, \\ \sigma_{\alpha,2}^{x,t,v,\omega}(s) & \text{if } s \geq t_l. \end{cases} \quad \text{(B.5)}$$

Let us first tackle the sampling of the interaction $\mathcal{S}$: such discontinuity can be handled with a simple process, given here for a particle at time $t < t_l$:

(i) sample interaction distance thanks to $\sigma_{\alpha,1}^{x,t,v,\omega}(s)$,

(ii) if the time is such that the particle position become greater than t_l ($s \geq t_l$) :

– then stop particle at $s = t_l$ and sample the interaction time thanks to $\sigma_{\alpha,2}^{x,t,v,\omega}(s)$.

This result is in fact very general and is due to the following property [19]:

Property 1 *Given $\mathcal{S}_1$ and $\mathcal{S}_2$ samples following the same generalized exponential law of probability density function $P_{\exp}(f(s)) = f(s)\exp(\int_0^s f(\beta)\,\mathrm{d}\beta)$, then $\forall t_l > 0$ and $\forall s > t_l$*

$$\mathbb{P}(\mathcal{S}_1 > s) = \mathbb{P}(\mathcal{S}_1 > t_l) \times \mathbb{P}(\mathcal{S}_2 > (s-t_l)).$$

Now, concerning particle weight modification $e^{-\int_{t-\mathcal{S}}^t v\sigma_a^{x,t,v,\omega}(\alpha)\,\mathrm{d}\alpha}$ in (B.4), we only introduce a sum of two indicatrices, namely $\sigma_a^{x,t,v,\omega}(\alpha) = \sigma_{a,1}^{x,t,v,\omega}(\alpha)\mathbf{1}_{[0,t_l]}(\alpha) + \sigma_{a,2}^{x,t,v,\omega}(\alpha)\mathbf{1}_{[t_l,t]}(\alpha)$, leading to

$$\exp\left(-\int_0^t v\sigma_a^{x,t,v,\omega}(\alpha)\,\mathrm{d}\alpha\right) = \exp\left(\int_0^t \left[\sigma_{a,1}^{x,t,v,\omega}(\alpha)\mathbf{1}_{[0,t_l]}(\alpha) + \sigma_{a,2}^{x,t,v,\omega}(\alpha)\mathbf{1}_{[t_l,t]}(\alpha)\right]\,\mathrm{d}\alpha\right), \quad \text{(B.6)}$$

$$\text{(B.7)}$$

The previous remarks where very general and independent of the time evolution of the characteristics $(\sigma_\alpha^{x,t,v,\omega}(s))_{\alpha\in\{s,t,R\}}$. We now suggest coming back to our particular framework, i.e. the introduction of the change of variable (26), so that (B.6) becomes

$$\begin{aligned}\exp\left(-\int_0^t v\sigma_a^{x,t,v,\omega}(\alpha)\,\mathrm{d}\alpha\right) &= \exp\left(\int_0^t \left[\partial_t \ln(z_1(x-v\omega\alpha,t-\alpha)\mathbf{1}_{[0,t_l]}(\alpha) + \partial_t \ln(z_2(x-v\omega\alpha,t-\alpha)\mathbf{1}_{[t_l,t]}(\alpha)\right]\,\mathrm{d}\alpha\right), \\ &\exp\left[\ln\left(\frac{z_1(x-v\omega t_l,t-t_l)}{z_1(x,0)}\right) + \ln\left(\frac{z_2(x-v\omega t,t)}{z_2(x-v\omega t_l,t-t_l)}\right)\right].\end{aligned}$$

As a consequence, in the case of constant characteristics within a cell, the spatial dependences drops and one can write

$$\begin{aligned} &\text{if} \quad \{\exists t_l\in[0,t]\,|\,s\in[0,t_l]\Rightarrow x_p\in\mathcal{D}_i \text{ and } s\in[t_l,t]\Rightarrow x_p\in\mathcal{D}_j\} \\ &\quad\text{then} \quad \exp\left(-\int_0^t v\sigma_a^{x,t,v,\omega}(\alpha)\,\mathrm{d}\alpha\right) = \frac{z_i(t_l)}{z_i(0)}\frac{z_j(t)}{z_j(t_l)}, \\ &\text{else} \\ &\quad\text{then} \quad \forall s\in[0,t], x_p\in\mathcal{D}_i \text{ and } \exp\left(-\int_0^t v\sigma_a^{x,t,v,\omega}(\alpha)\,\mathrm{d}\alpha\right) = \frac{z_i(t)}{z_i(0)}. \end{aligned} \quad \text{(B.8)}$$

Note that this treatment corresponds to the resolution of the free flight part in (25), i.e.

$$\partial_t f(x,t,\omega) + V\omega\nabla f(x,t,\omega) + \mathbf{Z^{-1}}(\mathbf{x},\mathbf{t})\mathbf{V}\omega\nabla\mathbf{Z}(\mathbf{x},\mathbf{t})f(x,t\omega) = 0. \quad \text{(B.9)}$$

References

[1] American Society of Mechanical Engineers ASME V&V 20-2009. Standard for Verification and Validation in Computational Fluid Dynamics and Heat Transfer. *ASME*, 2009.

[2] B. Brock, A. Belt, J. J. Billings, and M. Guidry. Explicit Integration with GPU Acceleration for Large Kinetic Networks. *submitted to J. Comp. Phys.*, arXiv:1409.5826[physics.comp-ph], 2015.

[3] Cacucci and Dan G. *Handbook of Nuclear Engineering*, volume 1. Springer Science & Business Media, 2010.

[4] M. Dahmani. *Résolution des équations de la cinétique des réacteurs par la méthode nodale mixte duale utilisant le modèle quasi-statique amélioré et implémentation dans le code CRONOS.* PhD thesis, Faculté des Sciences de Rabat, Maroc, 1999.

[5] J. Dufek and W. Gudowski. Stochastic approximation for Monte-Carlo Calculation of Steady-State Conditions in Thermal Reactors. *Nucl. Sci. Ener.*, 152:274–283, 2006.

[6] J. Dufek and V. Valtavirta. Time step length versus efficiency of Monte-Carlo burnup calculations. *Preprint submitted to Annals of Nuclear Energy*, 2014.

[7] Jan Dufek, Dan Kotlyar, and Eugene Shwageraus. Numerical stability of the predictor-corrector method in Monte Carlo burnup calculations of critical reactors. *Annals of Nuclear Energy*, 56:34–38, 2013.

[8] Jan Dufek, Dan Kotlyar, Eugene Shwageraus, and Jaakko Leppänen. The stochastic implicit Euler method: A stable coupling scheme for Monte Carlo burnup calculations. *Annals of Nuclear Energy*, 60:295–300, 2013.

[9] D. Dureau and G. Poëtte. Hybrid Parallel Programming Models for AMR Neutron Monte-Carlo Transport. In *Joint International Conference on Supercomputing in Nuclear Applications + Monte-Carlo*, number 04202 in Parallelism and HPC, Monte-Carlo, 2013.

[10] S. Glasstone G.I. Bell. *Nuclear Reactor Theory.* Van Nostrand Reinhold Company, New York, N.Y. 10001, 1970.

[11] A. Henry. The Application of Reactor Kinetics to the Analysis of Experiments. *Nucl. Sci. Engng*, 3:52–70, 1958.

[12] A. Henry and N.J Curlee. Verification of a Method for Treating Neutron Space-Time Problems. *Nucl. Sci. Engng*, 4:727–744, 1958.

[13] Aarno Isotalo. *Computational Methods for Burnup Calculations with Monte Carlo Neutronics* . PhD. Thesis, Aalto University School of Science Department of Applied Physics, 2013.

[14] A.E. Isotalo, J. Leppänen, and J. Dufek. Preventing Xenon Oscillations in Monte Carlo Burnup Calculations by Enforcing Equilibrium Xenon Distribution. *Annals of Nuclear Energy*, 60:78–85, 2013.

[15] B. Lapeyre, E. Pardoux, and R. Sentis. *Méthodes de Monte Carlo pour les équations de transport et de diffusion.* Number 29 in Mathématiques & Applications. Springer-Verlag, 1998.

[16] E. E. Lewis and W. F. Miller Jr. *Computational Methods of Neutron Transport.* John Wiley and Son New York, 1984.

[17] Cleve Moler and Charles Van Loan. Nineteen dubious ways to compute the exponential of a matrix, twenty-five years later. *SIAM REVIEW*, 45(1):3–000, 2003.

[18] K.O. Ott and D.A. Meneley. Accuracy of the Quasistatic Treatment of Spatial Reactor Kinetics. *Nucl. Sci. Engng*, 36(3):402–411, 1969.

[19] G. C. Papanicolaou. Asymptotic Analysis of Transport Processes. *Bulletin of the American Mathematical Society*, 81(2), 1975.

[20] C. Patricot. PhD thesis, to appear, 2016.

[21] C. Patricot, K. Ammar, G. Campioni, and E. Hourcade. Thermal-Hydraulic/Thermal-Mechanics Temporal Coupling for Unprotected Loss of Flow Accidents Simulations on a SFR. *Proc. Int. Conf. ICAPP, Nice (France), May 03-06*, 2015.

[22] C. Patricot, O. Fandeur, A.-M. Baudron, and D. Broc. Neutronic Calculation of Deformed Cores: Development of a Time-Dependent Diffusion Solver in CAST3M, A Mechanic Dedicated Finite Elements Code. *Proc. Int. Conf. PHYSOR 2016, Sun Valley, USA, May 01-05*, 2016.

[23] B. Perthame. *Transport Equations in Biology.* Birkhauser Verlag, Basel Boston Berlin, 2000.

[24] Fabiano S. Prata, Fernando C. Silva, and Aquilino S. Martinez. Solution of the Isotopic Depletion Equations using Decomposition Method and Analytical Solutions. *Progress in Nuclear Energy*, 69:53–58, 2013.

[25] J. Spanier and E. M. Gelbard. *Monte Carlo Principles and Neutron Transport Problems.* Addison-Wesley, 1969.